


Review

Advances in Designing Efficient La-Based Perovskites for the NO_x Storage and Reduction Process

Dongyue Zhao ¹, Haitao Song ¹, Jun Liu ¹, Qiuqiao Jiang ¹  and Xingang Li ^{2,*}

¹ Research Institute of Petroleum Processing, Sinopec, Beijing 100083, China; zhaodongyue.ripp@sinopec.com (D.Z.); songht.ripp@sinopec.com (H.S.); liujun.ripp@sinopec.com (J.L.); jiangqiuqiao.ripp@sinopec.com (Q.J.)

² Collaborative Innovation Center of Chemical Science and Engineering (Tianjin), Tianjin Key Laboratory of Applied Catalysis Science and Technology, School of Chemical Engineering and Technology, Tianjin University, Tianjin 300072, China

* Correspondence: xingang_li@tju.edu.cn

Abstract: To overcome the inherent challenge of NO_x reduction in the net oxidizing environment of diesel engine exhaust, the NO_x storage and reduction (NSR) concept was proposed in 1995, soon developed and commercialized as a promising DeNO_x technique over the past two decades. Years of practice suggest that it is a tailor-made technique for light-duty diesel vehicles, with the advantage of being space saving, cost effective, and efficient in NO_x abatement; however, the over-reliance of NSR catalysts on high loadings of Pt has always been the bottleneck for its wide application. There remains fervent interest in searching for efficient, economical, and durable alternatives. To date, La-based perovskites are the most explored promising candidate, showing prominent structural and thermal stability and redox property. The perovskite-type oxide structure enables the coupling of redox and storage centers with homogeneous distribution, which maximizes the contact area for NO_x spillover and contributes to efficient NO_x storage and reduction. Moreover, the wide range of possible cationic substitutions in perovskite generates great flexibility, yielding various formulations with interesting features desirable for the NSR process. Herein, this review provides an overview of the features and performances of La-based perovskite in NO oxidation, NO_x storage, and NO_x reduction, and in this way comprehensively evaluates its potential to substitute Pt and further improve the DeNO_x efficiency of the current NSR catalyst. The fundamental structure–property relationships are summarized and highlighted to instruct rational catalyst design. The critical research needs and essential aspects in catalyst design, including poisoner resistance and catalyst sustainability, are finally addressed to inspire the future development of perovskite material for practical application.

Keywords: NO_x removal; diesel engines exhaust; NO_x storage and reduction; perovskite; noble metals; sulfur tolerance



Citation: Zhao, D.; Song, H.; Liu, J.; Jiang, Q.; Li, X. Advances in Designing Efficient La-Based Perovskites for the NO_x Storage and Reduction Process. *Catalysts* **2022**, *12*, 593. <https://doi.org/10.3390/catal12060593>

Academic Editor:
Soghomon Boghosian

Received: 17 April 2022

Accepted: 23 May 2022

Published: 30 May 2022

Publisher's Note: MDPI stays neutral with regard to jurisdictional claims in published maps and institutional affiliations.



Copyright: © 2022 by the authors. Licensee MDPI, Basel, Switzerland. This article is an open access article distributed under the terms and conditions of the Creative Commons Attribution (CC BY) license (<https://creativecommons.org/licenses/by/4.0/>).

1. Introduction

The diesel engines operated under a high air-to-fuel (A/F) ratio in the range of 20 to 65 achieve higher fuel economy and better driving performance than the stoichiometric gasoline engines [1–3], but the higher combustion temperature and pressure in the diesel cylinder lead to increased NO_x emissions, and the net oxidizing environment of the exhaust brings huge challenges for NO_x reduction [2]. The conventional three-way catalysis (TWC) system developed for the removal of NO_x in gasoline engine exhaust is not as efficient as the A/F ratio shifts towards the lean-burn region. Thereafter, three alternative DeNO_x techniques were developed, that is, the direct decomposition of NO, selective catalytic reduction (SCR), and NO_x storage and reduction (NSR) or lean NO_x trap (LNT). NO decomposition in the absence of reductant was proposed as an ideal DeNO_x concept with thermodynamic feasibility, but was demonstrated to be kinetically sluggish, showing insufficient NO_x conversions that do not satisfy the requirements of real automotive emission

control systems [4,5]. However, the other two techniques have been fully developed and commercialized over the last several decades.

An SCR technique with ammonia from urea decomposition as the reductant was proposed in 1979, which was demonstrated to be efficient and selective for NO_x reduction to N₂ in net oxidizing atmosphere, especially in the temperature range of 250–450 °C [6–10]. However, the complex hardware system (including heated tanks and tubes, injector nozzle, and mixing device, to ensure storage and complete decomposition of urea, homogeneous flow distribution, and accurate dosing of NH₃) means that NH₃-SCR is not a suitable NO_x abatement technology for vehicles with space constraints and cost considerations [11]. The intrinsic risk of ammonium salt [(NH₄)₂SO₄] deposition and NH₃ slip also drove the exploration of novel NO_x removal techniques. Several research organizations then focused on the selective reduction of NO_x with hydrocarbons as the reductant in the 1990s, but this technique posed a couple of problems, including inadequate NO_x conversion and a narrow temperature window [12,13]. In this context, the NSR technique was proposed by Toyota in 1995 and is characteristic of incorporating basic components in DeNO_x catalyst formulation for NO_x storage, adopting alternating lean-burn/fuel-rich operations, and not requiring external reductants [14]. In the lean-burn periods of a typical NSR process, NO is oxidized to NO₂ and diffuses to the neighboring basic sites to form nitrates or nitrites species [15,16]. Then, the fuel or fuel-rich pulse is injected into the catalytic converter chamber to reduce the stored NO_x to N₂, thereby regenerating the occupied NO_x storage sites and preparing them for the next lean-burn period [15]. Adopting this alternating operation is a smart innovation to avoid the inherent challenge of NO_x reduction in the net oxidizing atmosphere.

An NSR system is ~50% space saving compared to NH₃-SCR [11], which exhibits qualified NO_x removal efficiency as well. NSR can also be applied to lean-burn gasoline engine vehicles or coupled with SCR, hence removing the urea injection system of SCR and making it more cost effective [17,18]. However, the application of NSR also suggests technical and cost concerns: (1) basic sites are irreversibly occupied by SO, so that long-term usage leads to continuous deactivation of the catalyst; and (2) high loadings of noble metals (mainly Pt) are demanded in commercial NSR catalysts to ensure sufficient NO oxidation and NO_x reduction efficiency in frequently switching operation mode [11,16]. To date, the former constraint has been greatly alleviated with the execution of increasingly stringent legislation to reduce automotive SO_x emissions, realized by the deep desulfurization of diesel by hydrotreating in refineries [19,20], while the challenges of high cost and low thermal stability of Pt have become the bottleneck for further application of NSR, and the attempts to find economical and durable alternatives have never stopped [11,16].

Perovskite-type oxide ABO₃ has been proven to be a promising candidate, with the advantage of high thermal stability, prominent redox property, and low cost [21–26]. In a cubic perovskite-type oxide ABO₃ with space group type Pm-3m, the A-site cation is 12-fold coordinated by oxygen anions, while the B-site cations are octahedrally coordinated (6-fold) [23]. A-site cations are large and generally basic, serving as NO_x storage sites; and B-site cations are small and chemically active, functioning as the redox center for NO oxidation and NO_x reduction [27–30]. The perovskite-type oxide structure of perovskite allows the integration of redox and storage components with homogeneous distribution and strong mutual interaction that substantially reduces the distance of NO_x diffusion, which is desirable for achieving a high lean-burn NO_x trapping rate and preventing fuel-rich NO_x slip, as compared to other NSR catalysts that are typically composed of multiple active metals/oxides and basic components with limited interface [31].

The perovskite possesses excellent compositional versatility, as it is able to accommodate nearly 90% of metals in the periodic table and form thermally stable oxides and able to endure partial cationic substitution, enabling flexible tuning of physio-chemical properties of the catalyst according to the reaction features [23,32–34]. Notably, any cation alternation or substitution can result in lattice expansion/shrinkage or a change in the extent of lattice distortion. For a specific formula, the selection of cations can refer to the tolerance factor

criterion, that is, $0.8 < (r_A + r_O) / [\sqrt{2}(r_B + r_O)] < 1$, which is reliable in most cases for predicting the structural stability of perovskite-type oxides [35]. Most of the research before 2010 investigated the perovskite simply as an NO_x storage material, as the substitute for BaO in a commercial NSR formulation. Alkaline-earth-metal-based perovskites, such as BaCeO₃, BaSnO₃, BaFeO₃, CaTiO₃, and SrTiO₃, were predominantly reported in this stage [36–42]. The main strategy was to use the perovskite-type oxide structure to modify sulfur- and sinter-resistant properties of the basic metals, whereas most of these formulations exhibited relatively inert redox properties and still required the addition of noble metals to facilitate NO oxidation and NO_x reduction. Over the last decade, La has gradually been accepted as an ideal option for A-site cation after extensive formulation screening. It was found to provide excellent structural thermal stability [3,16]. Most importantly, the proper ion radius of La³⁺ favors the accommodation of the transitional metals with prominent redox properties, such as Mn and Co. With the development of these perovskite formulations, noble metals have appeared less indispensable in NSR formulation.

In this review, we summarize the recent advances of the perovskites (mainly La-based) applied in the NSR field. Apart from highlighting the promising catalyst formulations and activity results, the review provides insights into the structure–property relationship that would instruct the rational design of perovskite-based NSR catalysts. Moreover, we disassemble the complex NSR reaction process into three general steps, that is, NO oxidation, NO_x storage/trapping, and NO_x desorption and reduction, and separately review the performance of perovskite catalysts in each step to provide deep and comprehensive perspectives on the advantages and potential problems of La-based perovskite employed in NSR reaction. The critical research needs are finally addressed for further development of this type of material.

2. NO Oxidation over La-Based Perovskites

NO oxidation to NO₂ as the first step of NO_x storage substantially impacts the overall storage efficiency in lean-burn periods [43,44], especially at low temperatures, when kinetic limitations dominate NO oxidation. This necessitates the incorporation of active oxidizing components, such as noble metals and perovskites, in NSR catalyst formulation. Over the Pt-based catalysts, NO oxidation was reported to proceed following the Langmuir–Hinshelwood (L-H) and/or Eley–Rideal (E-R) mechanism [45–47]. Both mechanisms describe O₂ adsorption and activation on noble metal clusters as the rate-limiting step of NO oxidation, but there is a divergence of opinion on whether the adsorbed NO on acid sites or gaseous NO takes part in the reaction. Weiss et al. [48,49] and Mulla et al. [50] pointed out that NO oxidation activity cannot be simply interpreted to be in inverse proportion to the cluster size of noble metal. Instead, a slight increase in cluster size decreased the binding energy of oxygen on coordinatively unsaturated Pt atoms, and thus increased the concentrations of oxygen vacancies and enhanced NO oxidation activity. However, long-term usage inevitably leads to the severe growth of Pt clusters and a dramatic activity decline. This motivates the later development of more thermally stable active centers for NO oxidation, such as perovskite.

Compared to noble metals, fewer mechanism studies have carried out on perovskites. Constantinou et al. [51] reported the reaction orders for NO₂, NO, and O₂ over LaMnO₃ to be around −1, 1, and 1, respectively, in accordance with the data collected over Pd- and Pt-based catalysts [49,52], which might indicate that NO oxidation over LaMnO₃ perovskite and noble metal catalysts share the same kinetic step. The negative reaction order of NO₂ implies a product inhibition effect. NO₂ strongly adsorbs on NO oxidation sites with a high sticking coefficient [50,53–56], thereby inhibiting NO adsorption and oxidation. Considering the compositional versatility of perovskite-based catalysts, the NO oxidation mechanism might vary as a function of the formulations. Besides L-H and E-R, the Mars–van Krevelen (MvK) mechanism might also function with lattice oxygen participating in the reaction.

As a general trend, perovskites possess comparable or even higher NO oxidation activity and much better durability than noble metal catalysts. He et al. [57] investigated the total substitution of Pt by LaCoO₃ perovskite in an NSR formulation and obtained an enhanced NO-to-NO₂ conversion of 38% over K₂CO₃/LaCoO₃/ZrTiO₄, compared to 18% over K₂CO₃/Pt/ZrTiO₄. The promising NO oxidation activity of the perovskite-based formulation was attributed to the low electron density in the d-orbit of Co³⁺, which was beneficial for accepting a lone pair on the N atom in NO. Afterwards, Chen et al. [58] also reported that the high oxidation state of B-site cations would be favorable for NO oxidation and identified the lattice oxygen bonded to Mn⁴⁺ as the active species. In this study, a series of nonstoichiometric La_xMnO₃ (0.9 < x < 1.11) catalysts were prepared. As the ratio of La/Mn decreased, the transformation of Mn³⁺ to Mn⁴⁺ was triggered to compensate for the charge imbalance caused by nonstoichiometry. As a concomitant of that, the NO-to-NO₂ conversion was promoted. As revealed in these studies, the high oxidation states of B-site cations, such as Co³⁺ and Mn⁴⁺, can be stabilized by a perovskite-type structure, which is considered a major reason for the superior oxidation activity of perovskite compared to single-transition metal oxides [59].

However, the B-site oxidation state does not always correlate well with activity trends. As a typical example, Li and coworkers [60] studied NO oxidation over Sr-doped LaCoO₃ and LaMnO₃ perovskites. The transformation of Mn³⁺ to Mn⁴⁺ induced by low-valence Sr²⁺ doping did not lead to a notable activity enhancement in this case. In contrast, the NO conversion over the LaCoO₃ increased from 69% to 86% at 300 °C after Sr doping. This was associated with the formation of oxygen vacancies in La_{0.9}Sr_{0.1}CoO₃, on which the weakly adsorbed oxygen species were highly active for NO oxidation. These observations were confirmed in a recent study by Onrubia et al. [61], which looked deeply into the effects of Sr doping on NO oxidation activity (Figure 1). They revealed that the amount of oxygen vacancies in the La_{1-x}Sr_xMnO₃ did not further increase as Sr substitution reached 10%, and the charge imbalance caused by further Sr doping was compensated by Mn⁴⁺ formation, which, however, did not promote the NO oxidation activity. On the other hand, the generation of oxygen vacancy appeared to be the only mechanism for charge neutralization of La_{1-x}Sr_xCoO₃. This leads to their conclusion that the amount of oxygen vacancies is the principal factor governing the NO oxidation activity of perovskites. In addition, Sr doping causes notable increases in the specific surface areas (SSA) of LaMnO₃ and LaCoO₃ perovskites.

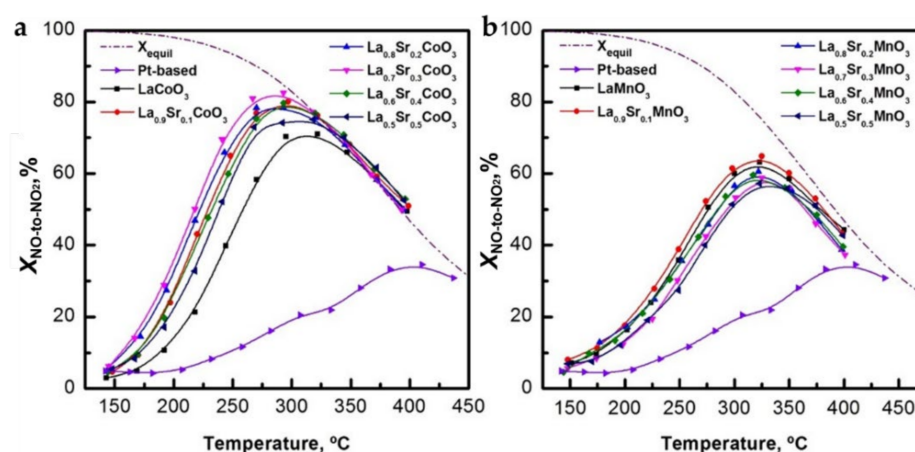


Figure 1. NO-to-NO₂ conversions over (a) La_{1-x}Sr_xCoO₃ and (b) La_{1-x}Sr_xMnO₃ perovskites with x ranging from 0 to 0.5, with model Pt-based catalyst as the benchmark. Adapted with permission from [61]. Copyright 2017, Elsevier.

Sr doping also alleviates the [CoO₆] octahedral distortion, and in some cases leads to the transition of the crystal structure of La-based perovskites from rhombohedral to cubic [62]. The Co³⁺ electronic configuration correspondingly switched from high/intermediate spin

state to low spin state with empty e_g filling. This favors the adsorption of electrophilic adsorbates, and hence enhances NO oxidation.

Ag^+ doping induced a more substantial charge imbalance than Sr^{2+} doping, which is beneficial to the formation of oxygen vacancies. With 10% of Ag doped into the A site of the LaMnO_3 perovskite, the activation energy for NO oxidation declined from 66.7 ± 2.1 to 47.9 ± 1.8 kJ mol^{-1} [63]. However, the maximum substitution amount of Ag in LaMnO_3 was only 20% at the A site.

Compared to A-site substitution, the alternation of B-site redox cations has a more direct impact on NO oxidation activity. Chen et al. [64] first investigated the activity of different B-site cations and provided the NO oxidation activity order of $\text{LaCoO}_3 > \text{LaMnO}_3 > \text{LaFeO}_3$, in accordance with the reducibility of the B-site cation. The results suggest that the adsorbed NO may react with lattice oxygen species. However, further examination reveals the inadequacies of such a simple correlation. For example, LaNiO_3 shows a higher reduction temperature than LaCoO_3 in H_2 -TPR, but a lower NO-to- NO_2 conversion [65]. In effect, when lattice oxygen participates in NO oxidation, this reaction is based on the cycling of reversible redox couples, such as $\text{Co}^{3+}/\text{Co}^{2+}$ and $\text{Mn}^{4+}/\text{Mn}^{3+}$, corresponding to the cyclic lattice oxygen storage and reaction process. Reducibility is apparently not enough to describe the cycling property, which is also determined by other factors, including the ability of the perovskite to host oxygen vacancies, filling rate of gaseous O_2 to oxygen vacancies, and lattice oxygen mobility [61]. Furthermore, in some reported perovskite systems, the adsorbed oxygen species appear more active for NO oxidation than lattice oxygen. For example, Zhong et al. [65] prepared a series of Co-doped LaNiO_3 perovskites by a co-precipitation approach. As a general trend, Co doping increased the NO and O_2 adsorption amount, and the adsorption strength of O_2 . The highest NO oxidation activity was observed over the $\text{LaNi}_{0.7}\text{Co}_{0.3}\text{O}_3$ catalyst, and this was ascribed to moderate adsorption strength and appropriate amount of adsorbed O_2 .

Besides transition metals, the perovskite structure allows the substitution of noble metals into the B site as well, but this is always limited to a trace amount due to cost considerations and ionic size disparity [66,67]. Pt doping generally promotes NO oxidation of perovskite since Pt itself is a highly active oxidation center. For example, $\text{LaCo}_{0.92}\text{Pt}_{0.08}\text{O}_3$ shows a higher NO-to- NO_2 conversion of 66.7% at 300 °C than the Pt-free counterpart of 42.0% [66], but the high Pt loading (~6.0 wt.%) makes the results less promising. Pd was demonstrated in our study to be less active than Pt in NO oxidation [67]. Only a slight increase in NO oxidation rate could be observed for Pd-doped $\text{La}_{0.7}\text{Sr}_{0.3}\text{CoO}_3$ perovskite compared to the Pd-free counterpart in the kinetic regime, and the Pd-supported perovskite even showed a lower NO oxidation activity. The kinetics show that the incorporation of Pd in either way does not alter the NO oxidation pathway. Perovskite continues to be the dominant oxidation center.

3. NO_x Storage

Upon NO being oxidized to NO_2 and diffused to neighboring basic sites, NO_x storage takes place on the catalyst surface, which is a unique behavior of NSR catalysts. Considering the essential impact of NO_x storage efficiency in lean-burn periods on overall DeNO_x activity, great efforts have been devoted to developing functional basic material that satisfies NO_x storage capacity (NSC) in a wide temperature window. Most of the studies before the year 2010 focused on single oxides with varying basicity, morphology, and interaction with supports, especially on the Pt/BaO/ Al_2O_3 model catalyst [11,16]. Perovskite accommodates basic metals in a complex oxide lattice with synergetic interaction with B-site cations, thus exhibiting new features for NO_x storage, distinct from the conventional basic components, which will be highlighted in this section with Pt/BaO/ Al_2O_3 as the benchmark.

Table 1 summarizes the NSC of La-based perovskite catalysts reported in the recent literature. Note that NSC cannot be simply described as an inherent attribute of the basic component, which is comprehensively affected by multiple factors [51]. As a general trend,

NSC varies with the temperature in a volcanic shape, restricted by insufficient NO-to-NO₂ conversions and sluggish NO_x diffusion at low temperatures (<250 °C), and by the loss of thermal stability of nitrates in the high-temperature region (>450 °C) [68]. With prominent NO oxidation ability, and a negligible NO_x diffusion barrier determined by the nature of the perovskite-type oxide structure, La-based perovskites generally exhibit higher NSC at low temperatures than the Pt/BaO/Al₂O₃ model catalyst, as observed over LaMn_{0.9}Fe_{0.1}O₃ and alumina-supported La_{0.5}Sr_{0.5}Fe_{1-x}Ti_xO_{3-δ} (Figure 2) [59,69], showing the potential to reduce the NO_x slip during cold start of the diesel engine, a long-lasting headache for automotive NO_x removal. Along this line, it should be mentioned that a prominent NO oxidation and NO_x storage performance was recently observed over Sr-based perovskites, such as Mn, Fe, Co-doped SrTiO₃ and SrFeO_{3-δ}, and Ruddlesden–Popper (RP)-type layered Sr₃Fe₂O_{7-δ} perovskite, in the low-temperature range [70–72], which was ascribed to the high mobility and reactivity of lattice oxygen. Among them, the Mn-doped SrTiO₃ exhibits a unique NO adsorption behavior at 323 K, that is, NO is adsorbed on the perovskite surface using lattice oxygens without the occurrence of NO oxidation, and this enables the catalyst to show significant NO_x storage capacity in a kinetically restricted temperature region for NO oxidation. The excellent NO_x storage performance at low temperatures makes them not only promising NSR catalysts, but also potential passive NO_x adsorber (PNA) materials.

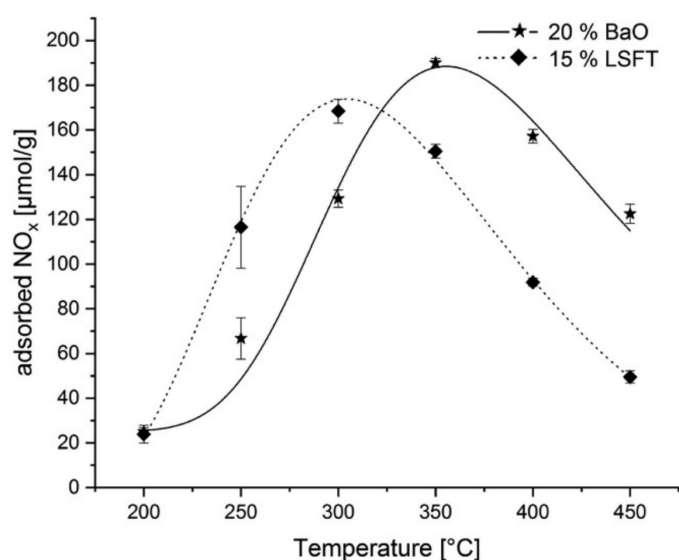


Figure 2. Comparison of the temperature-dependent NO_x storage capacities of infiltration composite 15 wt.% La_{0.5}Sr_{0.5}Fe_{1-x}Ti_xO_{3-δ} loading (◆) and a conventional Pt/BaO/Al₂O₃ (20% BaO) catalyst (★). Reprinted with permission from [59]. Copyright 2021, Elsevier.

At medium temperatures (250–450 °C), the NSC of Pt/BaO/Al₂O₃ substantially increases as a consequence of improved NO-to-NO₂ conversions (Figure 2). In comparison, the NSC of La-based perovskites appears less promising, especially for the LaCoO₃ and LaMnO₃ without cationic substitution, the NSCs of which were reported to be lower than 100 μmol g⁻¹ at 300 °C [73,74], as compared to ~140 μmol g⁻¹ for Pt/BaO/Al₂O₃ with 20% of Ba loadings, reported in [59]. Say et al. [75] investigated the NO_x adsorption behavior of these two perovskites using in situ infrared spectroscopy. The NO_x adsorption yielded multiple types of N-bearing species, including monodentate nitrite and nitrate, bidentate nitrate, bridging nitrate, and a small amount of bridging/chelating nitrites, but the free nitrate ions were not detected, suggesting that only surface La sites in perovskite are functional for NO_x storage. The inaccessibility of bulk storage sites can be ascribed to the high structural stability of La-based perovskite, which hinders the bulk phase transformation during NO_x adsorption and desorption [40]. This constitutes the major difference

between NO_x trapping on perovskites and on single basic oxides, that is, the latter allows the inward NO_x diffusion with phase transformation to nitrate [11]. The surface adsorption nature, to a large extent, accounts for the inadequate NSC of LaCoO_3 and LaMnO_3 perovskites at medium temperatures, even with the La-enriched surface [75], especially considering the poor texture property resulting from crystal growth of oxides at high calcination temperature. The surface areas of most proposed perovskites lie in the range of $5\text{--}20\text{ m}^2\text{ g}^{-1}$.

Aiming to improve NSC, additional alkali or alkaline earth metals are always incorporated in the perovskite formulation. For La-based perovskites, Sr is a common choice, since the doped Sr not only provides a stronger NO_x storage site on the surface, but also, as stated earlier, enhances NO oxidation activity and increases the surface area of the perovskite [61]. Our study [76] first investigated NO_x storage on Sr-doped LaCoO_3 perovskite through FT-IR and demonstrated three possible pathways (Figure 3): (1) NO_2 combines with surface lattice oxygen and forms monodentate nitrate; (2) NO_2 is directly trapped onto the oxygen vacancies and forms the “nitrate on perovskite” species; (3) NO_2 is trapped by segregated SrCO_3 and forms free nitrate ions. The presence of segregated SrCO_3 greatly increases NSC, and the nitrates formed on SrCO_3 show higher thermal stability than those on perovskite sites. After NO_x storage, a surface enrichment of Sr was observed, indicating possible exsolution of Sr^{2+} from the perovskite lattice and migration to the catalyst surface owing to the interaction with NO_x .

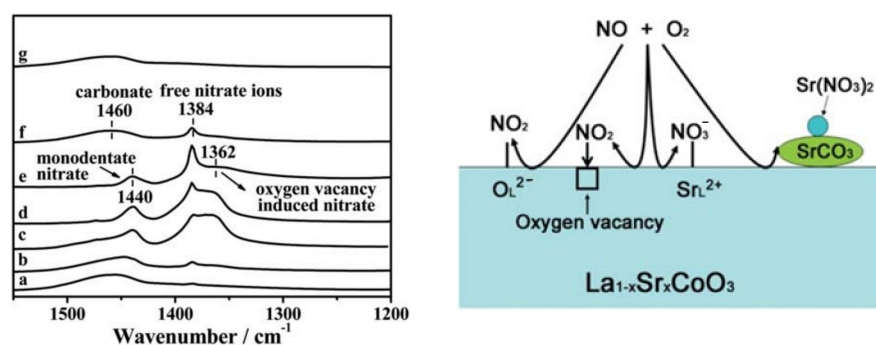


Figure 3. FT-IR spectra (left) of $\text{La}_{0.7}\text{Sr}_{0.3}\text{CoO}_3$: fresh (a); after NO_x storage at $200\text{ }^\circ\text{C}$ (b), $250\text{ }^\circ\text{C}$ (c), $300\text{ }^\circ\text{C}$ (d), $350\text{ }^\circ\text{C}$ (e), and $400\text{ }^\circ\text{C}$ (f); the sample (c) reduced by 5% H_2 at $300\text{ }^\circ\text{C}$ for 10 min (g). Possible NO_x storage routes on $\text{La}_{1-x}\text{Sr}_x\text{CoO}_3$ (right). Adapted from [76].

Dong et al. [77] substituted 30% of La with Sr and prepared $\text{La}_{0.7}\text{Sr}_{0.3}\text{MnO}_3$ via a sol-gel procedure under optimized synthesis conditions. The calcification velocity of $2\text{ }^\circ\text{C min}^{-1}$, calcination temperature of $700\text{ }^\circ\text{C}$, and pH of 8 were identified to favor the formation of pure perovskite phase and reduce particle aggregation, yielding the best NO oxidation and NO_x storage performance. Nonetheless, the best NSC of $\text{La}_{0.7}\text{Sr}_{0.3}\text{MnO}_3$ was only $170.4\text{ }\mu\text{mol g}^{-1}$ at $350\text{ }^\circ\text{C}$ (Table 1). As a comparison, the $\text{La}_{0.7}\text{Sr}_{0.3}\text{CoO}_3$ catalysts prepared via the same procedure present NSC in the range of $700.0\text{--}967.3\text{ }\mu\text{mol g}^{-1}$ [67,76]. In effect, the type of B-site cations affects the existing state of Sr. Compared to Mn-based perovskite, Co-based perovskite is less prone to accommodate Sr into perovskite lattice. The segregated SrCO_3 phase can always be detected in XRD patterns of $\text{La}_{1-x}\text{Sr}_x\text{CoO}_3$ [67,76].

Even though NSC is a significant descriptor for evaluating or predicting NO_x storage efficiency in lean-burn periods of NSR reaction, it only reflects the quantity of storage sites, rather than the quality. Indeed, the NSR reaction does not even demand huge NSC, but enough “reversible NO_x storage sites” that can rapidly trap NO_x and be effectively regenerated [67]. In this sense, compared to those sites embedded inside bulk, the surface sites are more desirable, since they skip the sluggish NO_x diffusion in the radial direction [31]. Along this line, efforts were devoted to exposing more surface storage sites of perovskite, and two strategies have proven effective.

(1) Preparing porous perovskite material. The construction of the porous structure of perovskite requires a hard or soft template. For example, Ye et al. [73] reported a nano-casting method for preparing mesoporous perovskite, with Santa Barbara Amorphous (SBA) as the hard template that was finally removed by NaOH solution. The as-prepared LaCoO_3 shows a high SSA of $75.0 \text{ m}^2 \text{ g}^{-1}$ and NSC of $252 \mu\text{mol g}^{-1}$, as compared to $93 \mu\text{mol g}^{-1}$ for the catalyst synthesized by the conventional sol-gel method. In a recent study, Xie et al. [78] also used the nano-casting method to synthesize mesoporous LaCoO_3 with KIT-6 as the hard template. The as-prepared LaCoO_3 -meso exhibits an even higher SSA of $246 \text{ m}^2 \text{ g}^{-1}$ and two times higher NSC compared to the counterpart prepared via the sol-gel method. More oxygen defects were produced on the surface of LaCoO_3 -meso with the confinement of the porous structure of the KIT-6 template, and this is revealed to improve oxygen mobility and favor fast NO_x storage and desorption. The majority of NO_x adsorbed on oxygen defects desorbed at low temperatures ($<240 \text{ }^\circ\text{C}$), indicating the weak basicity of such storage sites. Polymethyl methacrylate (PMMA) microspheres are the soft template generally used for synthesizing three-dimensionally ordered macroporous (3DOM) perovskite, and they can be completely removed by calcination. The as-prepared 3DOM perovskites are widely used for the simultaneous removal of soot and NO_x , since the macropores ($>50 \text{ nm}$) can accommodate soot particles ($<25 \text{ nm}$). However, for the application of porous perovskite materials, the mechanical strength and cost issues should be considered [23]

(2) Dispersing perovskite on oxide supports. This strategy has a simpler preparation procedure and is more commonly used. The properties of the support, to a large extent, affect the NO_x storage performance of perovskite. Supporting LaCoO_3 on ZrTiO_4 was found to be effective in improving NSC and reducing perovskite sintering [57]. Afterwards, You et al. [79,80] loaded 10% LaCoO_3 perovskite on CeO_2 and ternary $(\text{Y,Ce,Zr})\text{O}_2$ oxide supports. Despite the low loading, the catalyst achieved promising NO -to- NO_2 conversions and NSC, which was attributed to the high dispersion of perovskite and abundant surface-adsorbed oxygen species on the Ce-based support. More recently, Onrubia-Calvo et al. [81–83] conducted a series of studies comprehensively investigating the $\text{La}_{1-x}\text{Sr}_x\text{CoO}_3$ perovskite supported on Al_2O_3 , a cheap sinter-resistant support with a large surface area. At low loadings, Co preferably combined with Al_2O_3 and induced a solid phase transformation to CoAl_2O_4 ; high loadings benefited the formation of perovskite phase, but the less active bulk perovskite phase was also generated. Moreover, 30% perovskite loading on alumina was identified as an efficient formulation to balance dispersion and amount of active component (Figure 4), achieving a high NO_x storage capacity of $306 \mu\text{mol (g perovskite)}^{-1}$ at $400 \text{ }^\circ\text{C}$, compared to the bulky counterpart of $115 \mu\text{mol (g perovskite)}^{-1}$ [83]. The particle size of perovskite decreased from 50–150 nm to 20–50 nm in diameter after being supported on alumina. In a later study by Ecker et al. [59], alumina was again examined as support for perovskite. Fe was adopted as the B-site cation, partially doped by Nb, Ti, or Zr, to enhance sulfur resistance and phase stability. These catalysts, particularly $\text{La}_{0.5}\text{Sr}_{0.5}\text{Fe}_{1-x}\text{Ti}_x\text{O}_{3-\delta}$, exhibited promising hydrothermal stability, and the NSC decrease was less than 20% after aging at $750 \text{ }^\circ\text{C}$. To date, the most promising results were reported by an early study conducted by Ding et al. [84], obtained by loading $\text{La}_{0.7}\text{Sr}_{0.3}\text{CoO}_3$ on the mesoporous SiO_2 . The small crystalline size of perovskite confined in the mesoporous SiO_2 increased the surface area. The as-prepared catalyst has an SSA of $237.6 \text{ m}^2 \text{ g}^{-1}$, more than ten times higher than the perovskite prepared by the conventional sol-gel process ($18.7 \text{ m}^2 \text{ g}^{-1}$). The mesoporous SiO_2 -supported perovskite achieved an NSC of $5269.2 \mu\text{mol g}^{-1}$ in 3 h. Since NO oxidation activity was not substantially improved with the increase in SSA, in this case, the enhanced NSC was mainly related to the high dispersion of perovskite particles. Additionally, owing to the interactions between perovskite and mesoporous SiO_2 , the catalyst exhibited higher stability in the reducing atmosphere than perovskite prepared by the conventional sol-gel method.

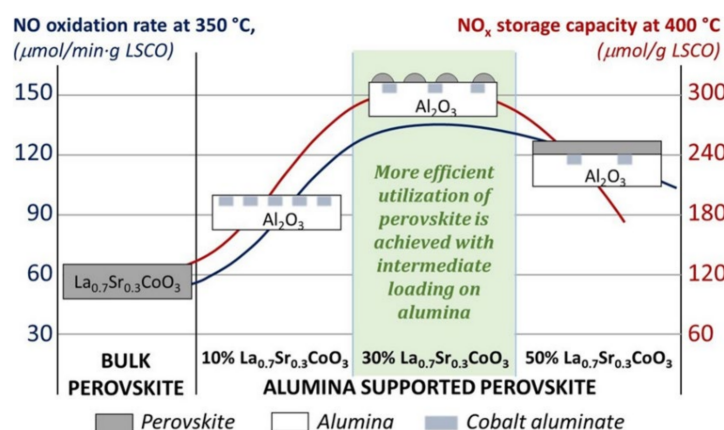


Figure 4. NO oxidation rate and NO_x storage capacity as functions of the loading of La_{0.7}Sr_{0.3}CoO₃ perovskite on alumina support. Reprinted with permission from [83]. Copyright 2019, Elsevier.

At high temperatures (>450 °C), the storage sites on La-based perovskite surface are basically not functional, due to the relatively weak basicity, which is unable to stabilize nitrates [59]. This further necessitates the incorporation of strong basic components into perovskite-based catalyst formulation [81]. Besides the aforementioned Sr-containing perovskites, various formulations were proposed along this line, such as 5% K₂CO₃ impregnated on mesoporous LaCoO₃ [73], Ba/Al₂O₃ ball-milled with LaMnO₃ [85], and La_xBa_{1-x}CoO₃ prepared via sol-gel procedure [86–88]. The results suggest that the high-temperature NSR performance was enhanced in the presence of these strong basic components. In fact, the Ba-based perovskite exhibits better high-temperature NO_x storage performance than the La-based counterparts, such as the BaTi_{0.8}Cu_{0.2}O₃ proposed in Albaladejo-Fuente’s study [89]. However, the Ba-based perovskite shows lower chemical and structural stability, as indicated by the phase segregation and transformation during the NO_x storage reaction [89]. Ba²⁺ in the A site is also less resistant to CO₂ in the atmosphere than La³⁺ due to the strong basicity, and hence it is more prone to exsolution from perovskite matrix to form a surface BaCO₃ layer [90]. These issues require special consideration in future studies, and the potential competitive or synergetic effect between different storage sites in NO_x adsorption or desorption at various temperatures needs to be specifically investigated.

Table 1. Review of NO_x storage capacity of the La-based perovskites.

Catalyst Formulation (Preparation Method)	Reaction Conditions	NO _x Storage, μmol g ⁻¹ (Temperature, °C)	Ref.
K ₂ O/LaCoO ₃ /ZrTiO ₄ (impregnation)	400 ppm NO/5% O ₂ /N ₂ ; GHSV = 60,000 mL g ⁻¹ h ⁻¹	325.0 (350)	[57]
Pt/La _{0.5} Sr _{0.5} Fe _{0.5} Ti _{0.5} O ₃ /Al ₂ O ₃ (impregnation)	500 ppm NO/500 ppm CO/200 ppm C ₃ H ₆ /9% H ₂ O/9% CO ₂ /6.5% O ₂ ; GHSV = 80,000 h ⁻¹	117.0 (250)	[59]
		150.0 (350)	
La _{0.7} Sr _{0.3} CoO ₃ (sol-gel)	400 ppm NO/ 5% O ₂ / balanced N ₂ ; GHSV = 120,000 mL g ⁻¹ h ⁻¹	50.0 (450)	[67]
		967.3 (300)	
LaMn _{0.9} Fe _{0.1} O ₃ (combustion)	500 ppm NO/8% O ₂ /N ₂ ; GHSV = 30,000 h ⁻¹	371.6 (100)	[69]
		392.3 (300)	
LaCoO ₃ (sol-gel)	400 ppm NO/5% O ₂ /N ₂ ; GHSV = 80,000 mL g ⁻¹ h ⁻¹	306.3 (400)	[73]
Mesoporous LaCoO ₃ (nano-casting)	400 ppm NO/5% O ₂ /N ₂ ; GHSV = 80,000 mL g ⁻¹ h ⁻¹	93.0 (350)	[73]
La _{0.7} Sr _{0.3} CoO ₃ (sol-gel)	800 ppm NO/5% O ₂ / N ₂ ; GHSV = 80,000 mL g ⁻¹ h ⁻¹	981.0 (350)	[76]
La _{0.7} Sr _{0.3} MnO ₃ (sol-gel)	800 ppm NO/5% O ₂ / N ₂ ; GHSV = 80,000 mL g ⁻¹ h ⁻¹	700.0 (300)	[77]
		170.4 (350)	

Table 1. Cont.

Catalyst Formulation (Preparation Method)	Reaction Conditions	NO _x Storage, μmol g ⁻¹ (Temperature, °C)	Ref.
K ₂ O/LaCoO ₃ /(Y,Ce,Zr)O ₂ (impregnation)	400 ppm NO/5% O ₂ /N ₂ ; GHSV = 45,000 h ⁻¹	639.0 (350)	[79]
LaCoO ₃ /3% K ₂ O/CeO ₂ (impregnation)	400 ppm NO/5% O ₂ /N ₂ ; GHSV = 45,000 h ⁻¹	512.4 (350)	[80]
30% Pd/La _{0.7} Sr _{0.3} CoO ₃ /Al ₂ O ₃ (impregnation)	500 ppm NO/6% O ₂ /Ar; GHSV = 123,500 h ⁻¹	97.3 (350)	[83]
La _{0.7} Sr _{0.3} CoO ₃ /mesoporous SiO ₂ (deposition)	500 ppm NO/ 5% O ₂ / N ₂ ; GHSV = 80,000 mL g ⁻¹ h ⁻¹	5269.2 (300)	[84]
La _{0.7} Sr _{0.3} CoO ₃ (sol-gel)	500 ppm NO/5% O ₂ / N ₂ ; GHSV = 80,000 mL g ⁻¹ h ⁻¹	2405.0 (300)	[84]

4. NO_x Desorption and Reduction

The engines are periodically shifted to fuel-rich conditions by introducing reductant pulses to regenerate the saturated storage sites, and NO_x is desorbed and reduced on the redox center. Since the desorption and the reduction occur in series in a rather short time, these two steps are basically inseparable and always examined in combination over the catalysts. Four factors mainly determine the efficiency of fuel-rich regeneration: (1) reaction temperature; (2) intrinsic reducing ability of the reductant (i.e., H₂ > CO > propene > propane); (3) stability of nitrate species, determined by the basicity of storage site; (4) redox property of the catalyst. In an early study [75], perovskite materials were found to be capable of activating N-O bonds at ca. 277 °C (even in the absence of reductants), with the formation of N₂ and N₂O as the NO_x decomposition products. This observation has long been considered to be an important indicator of La-based perovskites being promising catalysts for fuel-rich reactions. However, more detailed examinations revealed the deficiency of perovskite in NO_x reduction.

Table 2 summarizes the reaction conditions and DeNO_x activity of La-based perovskite catalysts in the recent literature. Our previous study [76] reported 71.4% DeNO_x activity and nearly 100% N₂ selectivity over the La_{0.7}Sr_{0.3}CoO₃ perovskite under alternating 3 min lean-burn/1 min fuel-rich conditions. However, only the NO_x species stored on perovskite sites were reduced in fuel-rich periods, while the saturated SrCO₃ site could hardly be regenerated, especially at low temperatures. Considering that such irreversible storage sites do not contribute to DeNO_x activity and may even cover the active sites on the surface, Peng et al. [91] used the diluted HNO₃ to remove the bulk SrCO₃ on La_{0.5}Sr_{0.5}CoO₃ perovskite, and observed a DeNO_x activity enhancement from 11.9 to 42.4% at 250 °C. These results indicate the mismatch between the strong basicity of SrCO₃ and relatively weak NO_x reduction ability of La-based perovskites. A-site cationic deficiency can also inhibit the formation of SrCO₃, which serves as an extra driving force for Sr doping into the perovskite structure, as observed with the La_{0.5}Sr_{0.3}MnO₃ catalyst in our study [31]. However, the DeNO_x activity of 43.2% over this catalyst at 350 °C was still insufficient for practical application, and the absence of strong basic sites inevitably leads to activity loss in the high-temperature region. It should be mentioned that the cationic deficiency affects the stability of the ABO₃ perovskite structure, and it can result in the formation of a complex layered intergrown structure and impurity phases [92], which should be carefully examined.

Shi [69] demonstrated that even with the excellent NO oxidation ability, the overall DeNO_x activity of LaMn_{0.9}Fe_{0.1}O₃ was still less than half that of conventional Pt/BaO/Al₂O₃ catalyst in the whole temperature range (30–400 °C), due to the weak NO_x reduction ability. In this case, a non-thermal H₂-plasma was employed to assist in activation of reductants in the fuel-rich periods (Figure 5a), and then an excellent DeNO_x activity of around 90% was achieved over perovskite with temperatures as low as 30 °C. Interestingly, the plasma did

not significantly improve the DeNO_x activity of the conventional Pt/BaO/Al₂O₃ catalyst, over which the rate-limiting step was NO oxidation and NO_x storage (Figure 5b,c).

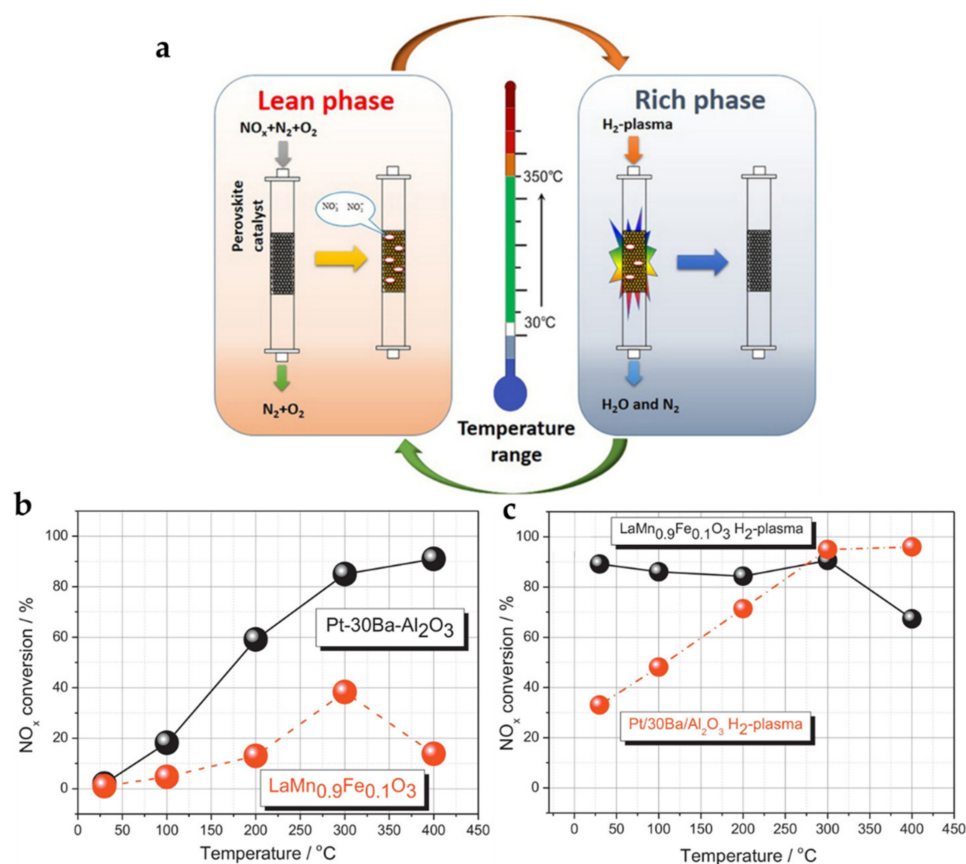


Figure 5. (a) Illustrative profile of NSR reaction with the assistance of H₂-plasma; NO_x conversion during lean/rich cycling at different temperatures over LaMn_{0.9}Fe_{0.1}O₃ and Pt/BaO/Al₂O₃: (b) without H₂-plasma, (c) with H₂-plasma. Reprinted with permission from [69]. Copyright 2013, Elsevier.

Even though the plasma technique provides great reinforcement for La-based perovskites, its application in a real aftertreatment system is restricted by cost constraints and product selectivity considerations. The noble metal is still required in the perovskite-based formulation to facilitate NO_x reduction. Wen et al. [93] synthesized a series of Pt/LaCoO₃/K₂O/Al₂O₃ with different Pt loadings (0, 0.3%, and 1.0%). On one hand, the addition of Pt enhanced the NO_x reduction ability of LaCoO₃/K₂O/Al₂O₃. On the other hand, the presence of LaCoO₃ increased the NO oxidation ability and NSC of Pt/K₂O/Al₂O₃, thereby reducing the Pt loading from 1.0% to 0.3% for achieving the equivalent DeNO_x activity in a wide temperature range (Figure 6). The combination of perovskite and a trace amount of noble metal seems to be a promising and economical formulation for efficient NO_x removal.

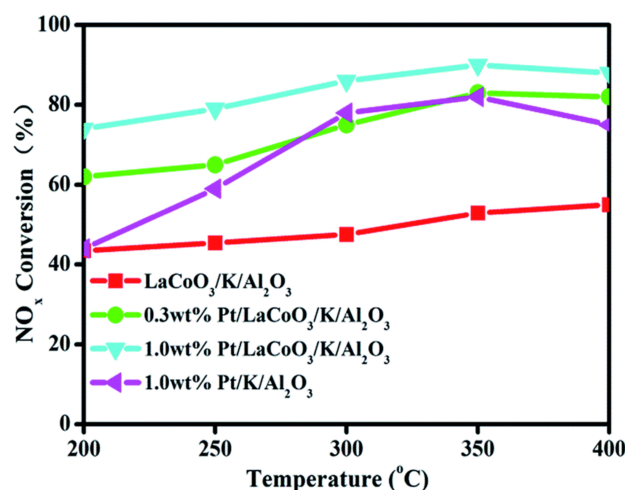


Figure 6. NO_x conversion of 1.0 wt.% Pt/K₂O/Al₂O₃ and *x* wt.% Pt/LaCoO₃/K₂O/Al₂O₃. Reprinted with permission from [93]. Copyright 2011, Royal Society of Chemistry.

Compared to Pt, Pd is more commonly used together with perovskite, due to the lower activation temperature for hydrocarbons and better thermal stability [94]. The inadequate NO oxidation ability of Pd will not be problematic when perovskite is present in a catalyst formulation. Nishihata et al. [95,96] proposed a famous intelligent Pd-doped perovskite catalyst (LaFe_{0.57}Co_{0.38}Pd_{0.05}O₃) in 2002 characterized by the “self-regeneration” of Pd, which showed the behavior of repeatedly moving into and out of the perovskite lattice in response to lean/rich atmospheric alternations, and in this way the particle growth could be suppressed. Along this line, Ueda et al. [97] added a basic component and prepared an La_{0.7}Ba_{0.3}Fe_{0.776}Nb_{0.194}Pd_{0.03}O₃ catalyst, which showed a DeNO_x activity of 47% at 250 °C. Afterwards, we reported [98] a La_{0.7}Sr_{0.3}Co_{0.97}Pd_{0.03}O₃ perovskite formulation prepared via the sol-gel method with comparable activity and selectivity to Pt-based catalyst. A combination of characterizations, including XRD, XPS, and EAXFS, were used to identify the dissolution of Pd into the perovskite lattice.

With the aim of achieving higher DeNO_x activity, in a more recent study, we investigated the optimal combination methods of perovskite and Pd by comparing the DeNO_x performance of doped Pd cation and PdO impregnated on perovskite surface [67]. As a general trend, both Pd species significantly promote the DeNO_x activity of La_{0.7}Sr_{0.3}CoO₃ perovskite by accelerating NO_x desorption and reduction. The impregnated PdO on the surface more effectively accelerated these steps due to the higher accessibility, and the efficient regeneration in turn increased NO_x storage efficiency in the lean-burn periods. The effects of the spatial locations of Pd species were confirmed in a later study by Onrubia et al. [84], which also demonstrated the poorer accessibility of Pd cations accommodated in perovskite structure. In this study, alumina was used as the support to disperse Pd and perovskite. The formulated 1.5% Pd/30% La_{0.7}Sr_{0.3}CoO₃/Al₂O₃ catalyst shows a prominent DeNO_x activity of 86.2% at 350 °C.

Besides the effect of spatial location, there is also debate concerning the active chemical state of Pd on perovskite, which is more complicated, because the chemical state may change dynamically during lean-burn/fuel-rich alternations. By properly tuning metal-support interactions, an interesting in situ activation behavior was observed over the Pd/La_{0.7}Sr_{0.3}MnO₃ catalyst in our study (Figure 7a) [99]. The DeNO_x activity substantially increased from 56.1% to 90.1%, with N₂O production simultaneously suppressed. This behavior resulted from the transformation of Pd²⁺ to Pd⁰ in the reaction atmosphere. The generated Pd⁰ showed a stronger ability to activate C₃H₆, and thus achieved eight-fold higher TOF for NO_x reduction than Pd²⁺ (Figure 7b). Notably, the excessive strength of interactions suppressed the in situ formation of Pd⁰, thus lowering the De-NO_x activity

even with high dispersion of Pd. These studies provide important information for designing efficient Pd-perovskite NSR catalysts.

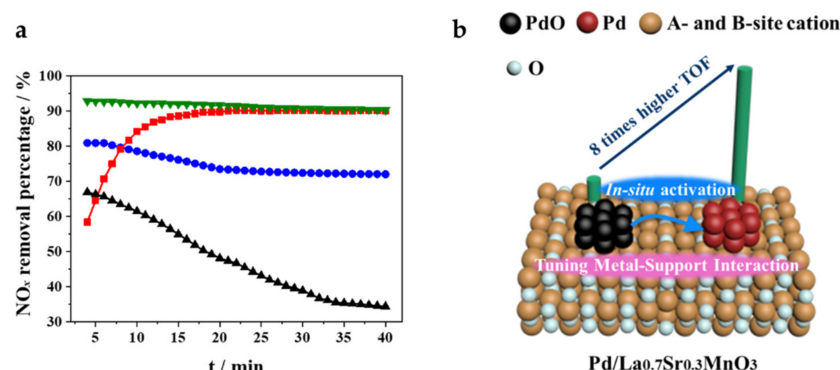


Figure 7. (a) De-NO_x activity as a function of reaction time at 350 °C of La_{0.7}Sr_{0.3}MnO₃ (▲), Pd/La_{0.7}Sr_{0.3}MnO₃-sol-gel (■), Pd/La_{0.7}Sr_{0.3}MnO₃-impregnation (●), and pretreated Pd/La_{0.7}Sr_{0.3}MnO₃-ol-gel (▼); and (b) illustrative profile of in situ activation of Pd/La_{0.7}Sr_{0.3}MnO₃-sol-gel catalyst. Adapted with permission from [99]. Copyright 2021, Elsevier.

Table 2. Review of the reaction conditions and DeNO_x activity of the La-based perovskites.

Catalyst (Preparation Method)	Reaction Conditions	DeNO _x Activity, % (Temperature, °C)	Ref.
La _{0.5} Sr _{0.3} MnO ₃ (sol-gel)	Lean (50 s): 400 ppm NO/5% O ₂ / N ₂ ; rich: phase (10 s): 1000 ppm C ₃ H ₆ /N ₂ ; GHSV = 120,000 mL g ⁻¹ h ⁻¹	43.2 (350)	[31]
LaCo _{0.92} Pt _{0.08} O ₃ (sol-gel)	Lean (120 s): 280 ppm NO/ 8% CO ₂ /3.5% H ₂ / N ₂ , GHSV = 72,000 h ⁻¹ (SO ₂ treatment: 100 ppm SO ₂ /8% O ₂ / N ₂ for 45 min; regeneration: 3.5 vol% H ₂ at 500 °C for 12 h)	90.9 (350) 25.5 (350, SO ₂ treatment) 75.5 (350, regeneration)	[66]
La _{0.7} Sr _{0.3} CoO ₃ (sol-gel)	Lean (50 s): 400 ppm NO/5% O ₂ / N ₂ ; rich (10 s): 1000 ppm C ₃ H ₆ /N ₂ ; GHSV = 120,000 mL g ⁻¹ h ⁻¹	51.6 (300)	[67]
La _{0.7} Sr _{0.3} Co _{0.97} Pd _{0.03} O ₃ (sol-gel)	Lean (50 s): 400 ppm NO/ 5% O ₂ /N ₂ ; rich (10 s): 1000 ppm C ₃ H ₆ /N ₂ ; GHSV = 120,000 mL g ⁻¹ h ⁻¹	74.4 (300)	[67]
1.4% Pd/La _{0.7} Sr _{0.3} CoO ₃ (impregnation)	Lean (50 s): 400 ppm NO/5% O ₂ /N ₂ ; rich (10 s): 1000 ppm C ₃ H ₆ / N ₂ ; GHSV = 120,000 mL g ⁻¹ h ⁻¹	90.4 (300)	[67]
LaMn _{0.9} Fe _{0.1} O ₃ (sol-gel)	Lean (10 min): 500 ppm NO/8% O ₂ /N ₂ ; rich (2 min): 1% H ₂ / N ₂ ; GHSV = 10,000 h ⁻¹ , plasma assisted Lean (3 min): 500 ppm NO/ 1000 ppm C ₃ H ₆ /6.7% O ₂ /N ₂ ; rich (1 min): 500 ppm NO/ 1000 ppm C ₃ H ₆ / N ₂ ; GHSV = 80,000 mL g ⁻¹ h ⁻¹	>80% (30–300)	[69]
LaCoO ₃ (sol-gel)	Lean (150 s): 500 ppm NO/6% O ₂ / Ar; rich (20 s): 512 ppm NO/ 3% H ₂ / Ar; GHSV = 123,500 mL g ⁻¹ h ⁻¹	71.4 (300)	[76]
1.5% Pd/30% La _{0.7} Sr _{0.3} CoO ₃ /Al ₂ O ₃ (impregnation)	Lean (3 min): 500 ppm NO/5% O ₂ / N ₂ ; rich (1 min): 500 ppm NO/1000 ppm C ₃ H ₆ / N ₂ ; GHSV = 120,000 mL g ⁻¹ h ⁻¹	86.2% (350)	[82]
La _{0.7} Sr _{0.3} CoO ₃ (sol-gel, acid wash)	Lean (120 s): 500 ppm NO/ 8% O ₂ / Ar ₂ , rich (120 s): 500 ppm NO/3.5% H ₂ / Ar; GHSV = 72,000 mL g ⁻¹ h ⁻¹	55.0% (300)	[91]
0.3% Pt/LaCoO ₃ /K ₂ O/Al ₂ O ₃ (impregnation)	Lean (54 s): 512 ppm NO/200 ppm C ₃ H ₆ /10% O ₂ / Ar; rich (6 s): 512 ppm NO/200 ppm C ₃ H ₆ /4% CO/ Ar; GHSV = 60,000 mL g ⁻¹ h ⁻¹	80.0 (300)	[93]
La _{0.7} Ba _{0.3} Fe _{0.776} Nb _{0.194} Pd _{0.03} O ₃ (glycine-nitrate method)	Lean (2 min): 0 or 100 ppm SO ₂ / 500 ppm NO/ 6.7% O ₂ / N ₂ ; rich (1 min): 0 or 100 ppm SO ₂ / 500 ppm NO/ 1000 ppm C ₃ H ₆ / N ₂ ; GHSV = 32,000 h ⁻¹	47.0 (250)	[97]
La _{0.7} Sr _{0.3} Co _{0.97} Pd _{0.03} O ₃ (sol-gel)	Lean (50 s): 400 ppm NO/5% O ₂ / N ₂ ; rich: phase (10 s): 1000 ppm C ₃ H ₆ / N ₂ ; GHSV = 120,000 mL g ⁻¹ h ⁻¹	100 (325) 99.2 (325, with SO ₂)	[98]
2.1%Pd/La _{0.7} Sr _{0.3} MnO ₃ (sol-gel)	Lean (50 s): 400 ppm NO/5% O ₂ / N ₂ ; rich: phase (10 s): 1000 ppm C ₃ H ₆ / N ₂ ; GHSV = 120,000 mL g ⁻¹ h ⁻¹	72.0 (350)	[99]
2.1%Pd/La _{0.7} Sr _{0.3} MnO ₃ (impregnation)	Lean (50 s): 400 ppm NO/5% O ₂ /N ₂ ; rich: phase (10 s): 1000 ppm C ₃ H ₆ /N ₂ ; GHSV = 120,000 mL g ⁻¹ h ⁻¹	90.1 (350)	[99]

5. Resistance to Poisoners

An inherent defect of NSR catalyst is the susceptibility to sulfur poisoning, due to the close binding affinity between basic components and SO_2 that easily leads to the formation of thermally stable sulfate, which causes the severe loss of NSC and continuous deactivation of the catalyst [11]. The sulfur tolerance is a major concern for the application of an NSR catalyst. Our recent studies illustrated that La-based perovskites had stronger sulfur tolerance than conventional $\text{Pd}/\text{BaO}/\text{Al}_2\text{O}_3$ and $\text{Pt}/\text{BaO}/\text{Al}_2\text{O}_3$ catalysts, which was tentatively assigned to the relatively weak basicity of perovskite storage sites and the stability of perovskite structure [31,99]. The incorporation of Fe into the B site of perovskite could further enhance the sulfur tolerance of La-based perovskite [100]. After the presulfation, the NSC of the $\text{La}_{0.7}\text{Sr}_{0.3}\text{CoO}_3$ dropped by 43.6%, while that of the $\text{La}_{0.7}\text{Sr}_{0.3}\text{Co}_{0.8}\text{Fe}_{0.2}\text{O}_3$ only dropped by 6.4%, since SO_2 preferentially bonded with Fe to form $\text{Fe}_2(\text{SO}_4)_3$, which circumvented the poisoning of the Sr site.

The regeneration of sulfated catalyst would be enhanced in the presence of noble metals. For example, Pd^0 species was revealed to be effective in reducing sulfur poisoning through promoting hydrogen spillover to regenerate adjacent sulfated storage sites before they developed into the irreducible bulk phase [98]. The DeNO_x activity of $\text{La}_{0.7}\text{Sr}_{0.3}\text{Co}_{0.97}\text{Pd}_{0.03}\text{O}_3$ declined from 100% to 70.2% after the presulfating treatment but was fully restored by H_2 reduction at a mild temperature (325°C). In contrast, the DeNO_x activity of $\text{Pt}/\text{BaO}/\text{Al}_2\text{O}_3$ catalyst declined from 99.2 to 54.9% and could not be recovered by H_2 reduction. The study also reveals that the sulfur species are less likely to deposit on the catalyst in the co-feeding condition, as compared to long-term sulfur pretreatment. However, once the bulk sulfate species form on the basic sites, they can hardly be regenerated in H_2 under 450°C . The influence of sulfur poisoning was also comparatively studied with $\text{Pt}/\text{BaO}/\text{Al}_2\text{O}_3$ and $\text{LaCo}_{0.92}\text{Pt}_{0.08}\text{O}_3$ [66]. Both catalysts suffered a drastic loss of NSC after a long-term presulfation (perovskite: 55.5 to $6.0\ \mu\text{mol g}^{-1}$, $\text{Pt}/\text{BaO}/\text{Al}_2\text{O}_3$: 53.9 to $2.9\ \mu\text{mol g}^{-1}$), as well as the decline of NO-to- NO_2 conversion. The recovery of NSC and NO oxidation activity of the catalysts by 3.5% H_2 reduction at 350°C was time dependent. A long regeneration time benefited the removal of sulfate species from the catalysts but led to the damage to perovskite structure. The perovskite catalyst exhibited better regenerability (Figure 8). This was assigned to the formation of reducible cobalt sulfate on perovskite, which is less stable than bulk BaSO_4 formed on $\text{Pt}/\text{BaO}/\text{Al}_2\text{O}_3$.

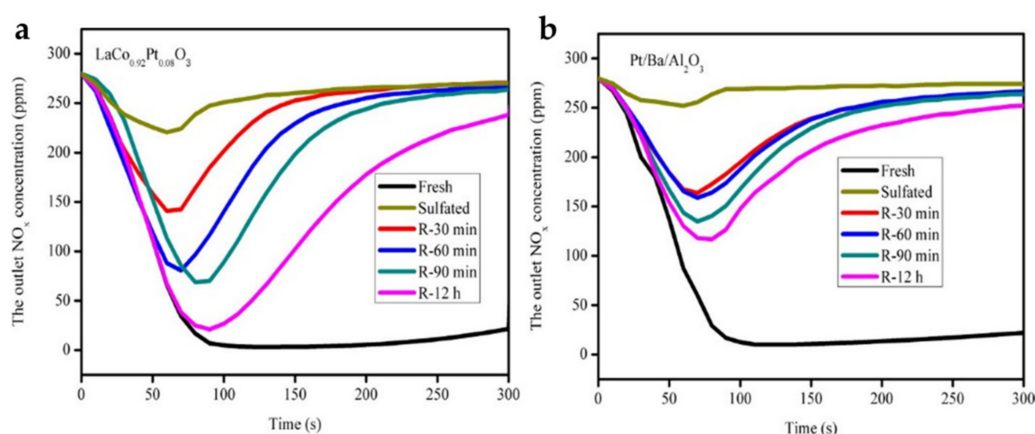


Figure 8. Outlet NO_x concentration at 350°C under lean conditions for fresh, sulfated, and regenerated (R) catalysts: (a) $\text{LaCo}_{0.92}\text{Pt}_{0.08}\text{O}_3$ and (b) $\text{Pt}/\text{BaO}/\text{Al}_2\text{O}_3$. Reprinted with permission from [66]. Copyright 2014, American Chemical Society.

H_2O is another poisoner for NSR catalysts and is known to impact NO_x storage performance via competitively adsorbing on basic sites, forming hydroxide [11]. Our study [99] revealed that compared with the conventional $\text{Pt}/\text{BaO}/\text{Al}_2\text{O}_3$ catalyst, the La-based perovskite showed slightly higher H_2O resistance, which was tentatively attributed to

the higher NO-to-NO₂ conversion [99], since NO₂ could be more easily stored on basic sites than NO. Different from SO₂, H₂O poisoning is reversible and less severe; the perovskite catalyst's activity can be gradually restored after shutting off the H₂O feed [66].

Besides SO₂ and H₂O, soot in the exhaust can also affect NSR performance. Toyota proposed a diesel particulate NO_x reduction (DPNR) filter system, which combines the functions of diesel particulate filter (DPF) and NSR and is operated under NSR cyclic conditions. Previous studies of Pt-based model NSR catalysts reveal that soot deposited on the surface of NSR catalyst reduces the NSC but promotes NO_x desorption and reduction [101]. However, there is a lack of research on perovskite-based catalysts for DPNR systems. Although some authors focus on the simultaneous removal of soot and NO_x with perovskite-based catalysts, they study the oxidation of soot and simultaneous reduction of NO_x [102,103]. This operation mode is very different from NSR.

6. Conclusions and Perspective

Diesel engines achieve lower fuel consumption and CO₂ emissions; however, the net oxidizing environment of exhaust is problematic for NO_x reduction. The conventional three-way catalysis designed for gasoline vehicles is not functional under lean-burn conditions, which drives the development of NSR and SCR techniques that basically cover different market niches. The NSR technique does not demand a complex hardware system to realize NO_x removal, so it is ideal for light-duty diesel vehicles with space constraints and cost considerations. However, NSR catalysts demand high loadings of Pt to achieve efficient NO_x removal, which adds to the cost and reduces the thermal stability of the catalysts. The La-based perovskites, considered an efficient, durable, and economical alternative to Pt, have been extensively researched over the past decade. Through comprehensively reviewing these reported formulations and activities, a global evaluation of La-based perovskite materials applied in the NSR process is provided.

Perovskite-type structure stabilizes the uncommonly high oxidation state of B-site cations, and thus exhibits significant NO oxidation activity, especially LaMnO₃ and LaCoO₃, which show even higher oxidation activity than Pt-based catalysts. This advantage is further strengthened by the partial substitution of A-site La by low-valence cations, such as Sr²⁺, Ag⁺, or Ba²⁺, since this triggers the formation of oxygen vacancies to neutralize charge imbalance. The prominent NO oxidation activity and eliminated NO_x diffusion barrier endow La-based perovskites with superior low-temperature NO_x storage capacity compared to conventional Pt/BaO/Al₂O₃, showing the potential to reduce the NO_x slip during cold start; however, at medium and high temperatures, La-based perovskites are less efficient for NO_x storage, which is ascribed to the surface adsorption nature, poor texture property, and relatively weak basicity of the La site. This motivates the adoption of various synthetic strategies to increase the exposed surface area of perovskite, and to incorporate stronger basic components into perovskite-based catalyst formulations. The major problem of La-based perovskites is the inadequate NO_x reduction performance in fuel-rich periods. This shows that the total substitution of noble metal by perovskite is not applicable. Nonetheless, a lower amount of noble metal is required in the presence of perovskite to reach the same DeNO_x performance, since perovskite covers the shortage in NO oxidation and low-temperature NSC of noble metal catalysts. The simultaneous use of perovskite and a trace amount of noble metal is proven to be a feasible strategy for achieving high DeNO_x activity in an economical way; therefore, how to increase the accessibility of noble metal and keep it in an active metallic state in a predominantly oxidizing atmosphere will be critical. Furthermore, the storage sites on La-based perovskite show strong sulfur tolerance, especially when Fe and Pd are incorporated. This increases the applicability to real automotive aftertreatment systems.

However, in-depth studies are still urgently needed for the future development of perovskite-based catalysts for NSR applications. The critical research areas and aspects that should be considered in future research mainly focus on the following aspects:

- (1) In-depth understanding of the NSR reaction mechanism in perovskites. To date, most mechanism studies concerning the NSR reaction were conducted with a Pt-based model catalyst, while for other types of catalysts, including perovskites, only vague pathways and plausible lines have been proposed. Considering the complexity of the reaction process, more in-depth experimental and theoretical studies should be conducted to unravel the detailed reaction routes, active sites, and intermediates to support the rational design of perovskite formulations with predictable properties.
- (2) Comprehensive comparison of NSR performance of La-based perovskites with others. The majority of perovskite-based materials reported for NSR applications over the last decade have been La-based. The obtained data reveals that La^{3+} provides prominent structural integrity with few impurities and little phase segregation, as well as thermal and chemical stability resistant to phase transformation during NO_x storage and reduction. Furthermore, the extensively studied LaCoO_3 and LaMnO_3 catalytic systems exhibit a good redox property, which is desirable for the NSR reaction. However, the weak basicity of A-site La^{3+} brings challenges for high-temperature NO_x storage, and the usage of La and Co increases environmental burdens from the perspective of sustainability. Some interesting data have been recently reported for Sr- and Ba-based perovskite formulations. On one hand, the stronger basicity of A-site alkaline earth metal provides better high-temperature NO_x storage performance, and the +2 oxidation state of the A-site cation increases the B-site oxidation state and/or generates oxygen vacancies desirable for NO oxidation and NO_x storage. On the other hand, these strongly basic cations are generally less resistant to CO_2 , NO_x , and SO_2 in the reaction atmosphere, and hence are prone to exsolution from the perovskite matrix, leading to the risk of collapse of the perovskite structure, but this tendency may vary depending on specific formulations. At this stage, a comprehensive study of the effects of different A-site cations on the activity and stability of perovskite catalysts in NSR reactions will be rather helpful.
- (3) Synergetic/competitive relation between different storage sites. As stated earlier, a practical NSR catalyst should be capable of efficiently trapping and releasing NO_x in a wide range of temperatures. This indicates that multiple storage components with different basicity should be used in combination; however, almost no comprehensive research has been devoted to this line. Current research suggests that La-based perovskite is an excellent low-temperature NO_x storage component, but whether the combination of perovskite and stronger basic sites efficient for high-temperature NSR reaction can work as they are intended remains unclear.
- (4) Redox stability and resistance to H_2O , CO_2 , and SO_2 poisoning. Most perovskite formulations are designed and tested under ideal laboratory conditions. The durability of perovskite catalysts in reducing atmosphere or when exposed to the common poisoners in automotive exhaust should be carefully considered and further clarified.
- (5) Sustainability has become an essential concern in catalyst design with the guidance of legislation and increasing environmental awareness of the community. However, this is entirely neglected in the currently reviewed publications. The environmental burden of using Pt on a per kilogram basis is calculated to be 3–4 orders of magnitude larger than base metals, in the aspects of global warming potential, cumulative energy demand, terrestrial acidification, freshwater eutrophication, and human toxicity [104], which necessitates the development of environmentally friendly base metal alternatives. Along this line, in perovskite formulation design, the metals at the lower end of the scale of environmental impacts should be preferably considered, such as manganese, iron, and titanium at B-site. These metals also result in decent NSR performance, while the usage of nickel and cobalt should be more prudent. For A-site cations, Sr and Ba are better choices than La.

Author Contributions: Conceptualization, D.Z.; formal analysis, D.Z., J.L. and Q.J.; writing—original draft preparation, D.Z.; writing—review and editing, X.L.; supervision, H.S.; project administration, H.S. All authors have read and agreed to the published version of the manuscript.

Funding: This work was supported by the Sinopec Research Program (119043 and 121011).

Acknowledgments: We acknowledge the inspiring discussion with Chunyu Xin and Zhongnan Gao in Tianjin University.

Conflicts of Interest: The authors declare no conflict of interest.

References

1. Bai, Z.F.; Zhang, Z.S.; Chen, B.B.; Zhao, Q.; Crocker, M.; Shi, C. Non-thermal plasma enhanced NSR performance over Pt/M/Ba/Al₂O₃ (M = Mn, Co, Cu) catalysts. *Chem. Eng. J.* **2017**, *314*, 688–699. [\[CrossRef\]](#)
2. Parks, J.E. Less costly catalysts for controlling engine emissions. *Science* **2010**, *327*, 1584–1585. [\[CrossRef\]](#) [\[PubMed\]](#)
3. Jabłońska, M.; Palkovits, R. Perovskite-based catalysts for the control of nitrogen oxide emissions from diesel engines. *Catal. Sci. Technol.* **2019**, *9*, 2057–2077. [\[CrossRef\]](#)
4. Zhang, Y.; Cao, G.; Yang, X. Advances in De-NO_x methods and catalysts for direct catalytic decomposition of NO: A review. *Energy Fuels* **2021**, *35*, 6443–6464. [\[CrossRef\]](#)
5. Ishihara, T.; Ando, M.; Sada, K.; Takiishi, K.; Yamada, K.; Nishiguchi, H.; Takita, Y. Direct decomposition of NO into N₂ and O₂ over La(Ba)Mn(In)O₃ perovskite oxide. *J. Catal.* **2003**, *220*, 104–114. [\[CrossRef\]](#)
6. Zhao, H.W.; Han, L.; Wang, Y.J.; Zheng, J.D. Insight into platinum poisoning effect on Cu-SSZ-13 in selective catalytic reduction of NO_x with NH₃. *Catalysts* **2021**, *11*, 796. [\[CrossRef\]](#)
7. Chen, C.; Cao, Y.; Liu, S.; Chen, J.; Jia, W. Review on the latest developments in modified vanadium-titanium-based SCR catalysts. *Chin. J. Catal.* **2018**, *39*, 1347–1365. [\[CrossRef\]](#)
8. Gao, F. Fe-exchanged small-pore zeolites as ammonia selective catalytic reduction (NH₃-SCR) catalysts. *Catalysts* **2020**, *10*, 1324. [\[CrossRef\]](#)
9. Sun, H.; Park, S. Recent advances in MnO_x/CeO₂-based ternary composites for selective catalytic reduction of NO_x by NH₃: A review. *Catalysts* **2021**, *11*, 1519. [\[CrossRef\]](#)
10. Zhao, X.; Mao, L.; Dong, G. Mn-Ce-V-WO_x/TiO₂ SCR catalysts: Catalytic activity, stability and interaction among catalytic oxides. *Catalysts* **2018**, *8*, 76. [\[CrossRef\]](#)
11. Roy, S.; Baiker, A. NO_x storage-reduction catalysis: From mechanism and materials properties to storage-reduction performance. *Chem. Rev.* **2009**, *109*, 4054–4091. [\[CrossRef\]](#)
12. Mrad, R.; Aissat, A.; Cousin, R.; Courcot, D.; Siffert, S. Catalysts for NO_x selective catalytic reduction by hydrocarbons (HC-SCR). *Appl. Catal. A* **2015**, *504*, 542–548. [\[CrossRef\]](#)
13. Liu, Z.; Ihl Woo, S. Recent advances in catalytic DeNO_x science and technology. *Catal. Rev.* **2006**, *48*, 43–89. [\[CrossRef\]](#)
14. Takahashi, N.; Shinjoh, H.; Iijima, T.; Suzuki, T.; Yamazaki, K.; Yokota, K.; Suzuki, H.; Miyoshi, N.; Matsumoto, S.; Tanizawa, T.; et al. The new concept 3-way catalyst for automotive lean-burn engine: NO_x storage and reduction catalyst. *Catal. Today* **1996**, *27*, 63–69. [\[CrossRef\]](#)
15. Yin, M.X.; Liu, D.S.; Zhao, D.Y.; Ding, T.; Tian, Y.; Li, X.G. Effect of copper doping on lean NO_x Trap Performance of Pt/Ba/Cu_xMg_{1-x}Al₂O₄ catalysts at high temperatures. *Chem. J. Chin. Univ.* **2019**, *40*, 2170–2177.
16. Epling, W.S.; Campbell, L.E.; Yezerets, A.; Currier, N.W.; Parks, J.E. Overview of the fundamental reactions and degradation mechanisms of NO_x storage/reduction catalysts. *Catal. Rev.* **2004**, *46*, 163–245. [\[CrossRef\]](#)
17. Park, C.; Lee, S.; Yi, U. Effects of engine operating conditions on particle emissions of lean-burn gasoline direct-injection engine. *Energy* **2016**, *115*, 1148–1155. [\[CrossRef\]](#)
18. Praveena, V.; Martin, M.L.J. A review on various after treatment techniques to reduce NO_x emissions in a CI engine. *J. Energy Inst.* **2018**, *91*, 704–720. [\[CrossRef\]](#)
19. Song, C. An overview of new approaches to deep desulfurization for ultra-clean gasoline, diesel fuel and jet fuel. *Catal. Today* **2003**, *86*, 211–263. [\[CrossRef\]](#)
20. Pérot, G. Hydrotreating catalysts containing zeolites and related materials-mechanistic aspects related to deep desulfurization. *Catal. Today* **2003**, *86*, 111–128. [\[CrossRef\]](#)
21. Yang, X.; Gao, Q.; Zhao, Z.; Guo, Y.; Guo, Y.; Wang, L.; Wang, Y.; Zhan, W. Surface tuning of noble metal doped perovskite oxide by synergistic effect of thermal treatment and acid etching: A new path to high-performance catalysts for methane combustion. *Appl. Catal. B* **2018**, *239*, 373–382. [\[CrossRef\]](#)
22. Xu, J.; Liu, J.; Zhao, Z.; Zheng, J.; Zhang, G.; Duan, A.; Jiang, G. Three-dimensionally ordered macroporous LaCo_xFe_{1-x}O₃ perovskite-type complex oxide catalysts for diesel soot combustion. *Catal. Today* **2010**, *153*, 136–142. [\[CrossRef\]](#)
23. Hwang, J.; Rao, R.R.; Giordano, L.; Katayama, Y.; Yu, Y.; Shao-Horn, Y. Perovskites in catalysis and electrocatalysis. *Science* **2017**, *358*, 751–756. [\[CrossRef\]](#) [\[PubMed\]](#)
24. Peng, Y.; Si, W.; Li, J.; Crittenden, J.; Hao, J. Experimental and DFT studies on Sr-doped LaMnO₃ catalysts for NO_x storage and reduction. *Catal. Sci. Technol.* **2015**, *5*, 2478–2485. [\[CrossRef\]](#)

25. Li, F.; Tang, J.; Ke, Q.; Guo, Y.; Ha, M.N.; Wan, C.; Lei, Z.; Gu, J.; Li, Q.; Nguyen, V.N.; et al. Investigation into enhanced catalytic performance for epoxidation of styrene over $\text{LaSrCo}_x\text{Fe}_{2-x}\text{O}_6$ double perovskites: The role of singlet oxygen species promoted by the photothermal effect. *ACS Catal.* **2021**, *11*, 11855–11866. [[CrossRef](#)]
26. Si, W.; Wang, Y.; Peng, Y.; Li, J. Selective dissolution of A-site cations in ABO_3 perovskites: A new path to high-performance catalysts. *Angew. Chem.* **2015**, *127*, 8065–8068. [[CrossRef](#)]
27. Gao, Z.N.; Guo, L.H.; Zhao, D.Y.; Li, X.G. Effect of A site-deficiency on the structure and catalytic oxidation activity of the La-Sr-Co-O perovskite. *Chem. J. Chin. Univ.* **2021**, *42*, 2869–2877.
28. Hernández-Giménez, A.; Castelló, D.; Bueno-López, A. Diesel soot combustion catalysts: Review of active phases. *Chem. Pap.* **2014**, *68*, 1154–1168. [[CrossRef](#)]
29. Zhu, J.; Thomas, A. Perovskite-type mixed oxides as catalytic material for NO removal. *Appl. Catal. B* **2009**, *92*, 225–233. [[CrossRef](#)]
30. Royer, S.; Duprez, D.; Can, F.; Courtois, X.; Batiot-Dupeyrat, C.; Laassiri, S.; Alamdari, H. Perovskites as substitutes of noble metals for heterogeneous catalysis: Dream or reality. *Chem. Rev.* **2014**, *114*, 10292–10368. [[CrossRef](#)]
31. Zhao, D.Y.; Yang, Y.X.; Gao, Z.N.; Tian, Y.; Zhang, J.; Jiang, Z.; Li, X.G. A-site defects in perovskite-based catalyst promoting NO_x storage and reduction for lean-burn exhausts. *J. Rare Earth* **2021**, *39*, 959–968. [[CrossRef](#)]
32. Švarcová, S.; Wiik, K.; Tolchard, J.; Bouwmeester, H.J.; Grande, T. Structural instability of cubic perovskite $\text{Ba}_x\text{Sr}_{1-x}\text{Co}_{1-y}\text{Fe}_y\text{O}_{3-\delta}$. *Solid State Ion.* **2008**, *178*, 1787–1791. [[CrossRef](#)]
33. Zhu, J.; Li, H.; Zhong, L.; Xiao, P.; Xu, X.; Yang, X.; Zhao, Z.; Li, J. Perovskite oxides: Preparation, characterizations, and applications in heterogeneous catalysis. *ACS Catal.* **2014**, *4*, 2917–2940. [[CrossRef](#)]
34. Labhassetwar, N.; Saravanan, G.; Megarajan, S.K.; Manwar, N.; Khobragade, R.; Doggali, P.; Grasset, F. Perovskite-type catalytic materials for environmental applications. *Sci. Technol. Adv. Mater.* **2015**, *16*, 036002. [[CrossRef](#)]
35. Li, C.; Soh, K.C.K.; Wu, P. Formability of ABO_3 perovskites. *J. Alloy Compd.* **2004**, *372*, 40–48. [[CrossRef](#)]
36. Xian, H.; Zhang, X.; Li, X.; Li, L.; Zou, H.; Meng, M.; Li, Q.; Tan, Y.; Tsubaki, N. BaFeO_{3-x} perovskite: An efficient NO_x absorber with a high sulfur tolerance. *J. Phys. Chem. C* **2010**, *114*, 11844–11852. [[CrossRef](#)]
37. Xian, H.; Zhang, X.W.; Li, X.G.; Zou, H.H.; Meng, M.; Zou, Z.Q.; Guo, L.H.; Tsubaki, N. Effect of the calcination conditions on the NO_x storage behavior of the perovskite BaFeO_{3-x} catalysts. *Catal. Today* **2010**, *158*, 215–219. [[CrossRef](#)]
38. Xian, H.; Li, F.L.; Li, X.G.; Zhang, X.W.; Meng, M.; Zhang, T.Y.; Tsubaki, N. Influence of preparation conditions to structure property, NO_x and SO_2 sorption behavior of the BaFeO_{3-x} perovskite catalyst. *Fuel Process. Technol.* **2011**, *92*, 1718–1724. [[CrossRef](#)]
39. Ge, C.; Li, L.; Xian, H.; Yan, H.; Meng, M.; Li, X. Effects of Ti-doping on the NO_x storage and the sulfur resistance of the $\text{BaFe}_{1-x}\text{Ti}_x\text{O}_{3-y}$ perovskite-type catalysts for lean-burn exhausts. *Fuel Process. Technol.* **2014**, *120*, 1–7. [[CrossRef](#)]
40. Hodjati, S.; Vaezzadeh, K.; Petit, C.; Pitchon, V.; Kiennemann, A. Absorption/desorption of NO_x process on perovskites: Performances to remove NO_x from a lean exhaust gas. *Appl. Catal. B* **2000**, *26*, 5–16. [[CrossRef](#)]
41. Hodjati, S.; Petit, C.; Pitchon, V.; Kiennemann, A. Absorption/desorption of NO_x process on perovskites: Impact of SO_2 on the storage capacity of BaSnO_3 and strategy to develop thioresistance. *Appl. Catal. B* **2001**, *30*, 247–257. [[CrossRef](#)]
42. Li, X.; Chen, J.; Lin, P.; Meng, M.; Fu, Y.; Tu, J.; Li, Q. A study of the NO_x storage catalyst of Ba-Fe-O complex oxide. *Catal. Commun.* **2004**, *5*, 25–28. [[CrossRef](#)]
43. Olsson, L.; Persson, H.; Fridell, E.; Skoglundh, M.; Andersson, B. A kinetic study of NO oxidation and NO_x storage on Pt/ Al_2O_3 and Pt/ $\text{BaO}/\text{Al}_2\text{O}_3$. *J. Phys. Chem. B* **2001**, *105*, 6895–6906. [[CrossRef](#)]
44. Bhatia, D.; McCabe, R.W.; Harold, M.P.; Balakotiah, V. Experimental and kinetic study of NO oxidation on model Pt catalysts. *J. Catal.* **2009**, *266*, 106–119. [[CrossRef](#)]
45. Hauff, K.; Tüttles, U.; Eigenberger, G.; Nieken, U. Platinum oxide formation and reduction during NO oxidation on a diesel oxidation catalyst—experimental results. *Appl. Catal. B* **2012**, *123*, 107–116. [[CrossRef](#)]
46. Li, L.D.; Shen, Q.; Cheng, J.; Hao, Z.P. Catalytic oxidation of NO over TiO_2 supported platinum clusters. II: Mechanism study by in situ FTIR spectra. *Catal. Today* **2010**, *158*, 361–369. [[CrossRef](#)]
47. Hong, Z.; Wang, Z.; Li, X.B. Catalytic oxidation of nitric oxide (NO) over different catalysts: An overview. *Catal. Sci. Technol.* **2017**, *7*, 3440–3452. [[CrossRef](#)]
48. Weiss, B.M.; Iglesia, E. NO oxidation catalysis on Pt clusters: Elementary steps, structural requirements, and synergistic effects of NO_2 adsorption sites. *J. Phys. Chem. C* **2009**, *113*, 13331–13340. [[CrossRef](#)]
49. Weiss, B.M.; Iglesia, E. Mechanism and site requirements for NO oxidation on Pd catalysts. *J. Catal.* **2010**, *272*, 74–81. [[CrossRef](#)]
50. Mulla, S.S.; Chen, N.; Cumarantunge, L.; Blau, G.E.; Zemlyanov, D.Y.; Delgass, W.N.; Epling, W.S.; Ribeiro, F.H. Reaction of NO and O_2 to NO_2 on Pt: Kinetics and catalyst deactivation. *J. Catal.* **2006**, *241*, 389–399. [[CrossRef](#)]
51. Constantinou, C.; Li, W.; Qi, G.; Epling, W.S. NO_x storage and reduction over a perovskite-based lean NO_x trap catalyst. *Appl. Catal. B* **2013**, *134*, 66–74. [[CrossRef](#)]
52. Mulla, S.S.; Chen, N.; Delgass, W.N.; Epling, W.S.; Ribeiro, F.H. NO_2 inhibits the catalytic reaction of NO and O_2 over Pt. *Catal. Lett.* **2005**, *100*, 267–270. [[CrossRef](#)]
53. Sivachandiran, L.; Thévenet, F.; Gravejat, P.; Rousseau, A. Investigation of NO and NO_2 adsorption mechanisms on TiO_2 at room temperature. *Appl. Catal. B* **2013**, *142*, 196–204. [[CrossRef](#)]
54. Epling, W.S.; Parks, J.E.; Campbell, G.C.; Yezerets, A.; Currier, N.W.; Campbell, L.E. Further evidence of multiple NO_x sorption sites on NO_x storage/reduction catalysts. *Catal. Today* **2004**, *96*, 21–30. [[CrossRef](#)]

55. Parker, D.H.; Koel, B.E. Chemisorption of high coverages of atomic oxygen on the Pt (111), Pd (111), and Au (111) surfaces. *J. Vac. Sci. Technol. A* **1990**, *8*, 2585–2590. [[CrossRef](#)]
56. Segner, J.; Vielhaber, W.; Ertl, G. Interaction of NO₂ with a Pt (111) surface. *Isr. J. Chem.* **1982**, *22*, 375–379. [[CrossRef](#)]
57. He, X.; Meng, M.; He, J.; Zou, Z.; Li, X.; Li, Z.; Jiang, Z. A potential substitution of noble metal Pt by perovskite LaCoO₃ in ZrTiO₄ supported lean-burn NO_x trap catalysts. *Catal. Commun.* **2010**, *12*, 165–168. [[CrossRef](#)]
58. Chen, J.; Shen, M.; Wang, X.; Qi, G.; Wang, J.; Li, W. The influence of nonstoichiometry on LaMnO₃ perovskite for catalytic NO oxidation. *Appl. Catal. B* **2013**, *134*, 251–257. [[CrossRef](#)]
59. Ecker, S.I.; Dornseiffer, J.; Werner, J.; Schlenz, H.; Sohn, Y.J.; Sauerwein, F.S.; Baumann, S.; Bouwmeester, H.J.M.; Guillon, O.; Weirich, T.E.; et al. Novel low-temperature lean NO_x storage materials based on La_{0.5}Sr_{0.5}Fe_{1-x}M_xO_{3-δ}/Al₂O₃ infiltration composites (M = Ti, Zr, Nb). *Appl. Catal. B* **2021**, *286*, 119919. [[CrossRef](#)]
60. Kim, C.H.; Qi, G.; Dahlberg, K.; Li, W. Strontium-doped perovskites rival platinum catalysts for treating NO_x in simulated diesel exhaust. *Science* **2010**, *327*, 1624–1627. [[CrossRef](#)]
61. Onrubia, J.A.; Pereda-Ayo, B.; De-La-Torre, U.; González-Velasco, J.R. Key factors in Sr-doped LaBO₃ (B = Co or Mn) perovskites for NO oxidation in efficient diesel exhaust purification. *Appl. Catal. B* **2017**, *213*, 198–210. [[CrossRef](#)]
62. Guo, L.H.; Bo, L.; Li, Y.; Jiang, Z.; Tian, Y.; Li, X.G. Sr doping effect on the structure property and NO oxidation performance of dual-site doped perovskite La(Sr)Co(Fe)O₃. *Solid State Sci.* **2021**, *113*, 106519. [[CrossRef](#)]
63. Lim, E.; Kim, Y.J.; Kim, J.H.; HoKim, J.; Ryu, T.; Lee, S.; Cho, B.K.; Nam, I.; Choung, J.W.; Yoo, S. NO oxidation activity of Ag-doped perovskite catalysts. *J. Catal.* **2014**, *319*, 182–193.
64. Chen, J.; Shen, M.; Wang, X.; Wang, J.; Su, Y.; Zhao, Z. Catalytic performance of NO oxidation over LaMeO₃ (Me = Mn, Fe, Co) perovskite prepared by the sol-gel method. *Catal. Commun.* **2013**, *37*, 105–108. [[CrossRef](#)]
65. Zhong, S.; Sun, Y.; Xin, H.; Yang, C.; Chen, L.; Li, X. NO oxidation over Ni-Co perovskite catalysts. *Chem. Eng. J.* **2015**, *275*, 351–356. [[CrossRef](#)]
66. Wang, X.; Qi, X.; Chen, Z.; Jiang, L.; Wang, R.; Wei, K. Studies on SO₂ tolerance and regeneration over perovskite-type LaCo_{1-x}Pt_xO₃ in NO_x storage and reduction. *J. Phys. Chem. C* **2014**, *118*, 13743–13751. [[CrossRef](#)]
67. Zhao, D.; Gao, Z.; Xian, H.; Xing, L.; Yang, Y.; Tian, Y.; Ding, T.; Jiang, Z.; Zhang, J.; Zheng, L.R.; et al. Addition of Pd on La_{0.7}Sr_{0.3}CoO₃ perovskite to enhance catalytic removal of NO_x. *Ind. Eng. Chem. Res.* **2018**, *57*, 521–531. [[CrossRef](#)]
68. Epling, W.S.; Yezerets, A.; Currier, N.W. The effects of regeneration conditions on NO_x and NH₃ release from NO_x storage/reduction catalysts. *Appl. Catal. B* **2007**, *74*, 117–129. [[CrossRef](#)]
69. Shi, C.; Zhang, Z.; Crocker, M.; Xu, L.; Wang, C.Y.; Au, C.; Zhu, A.M. Non-thermal plasma-assisted NO_x storage and reduction on a LaMn_{0.9}Fe_{0.1}O₃ perovskite catalyst. *Catal. Today* **2013**, *211*, 96–103. [[CrossRef](#)]
70. Yoshiyama, Y.; Hosokawa, S.; Tamai, K.; Kajino, T.; Yoto, H.; Asakura, H.; Teramura, K.; Tanaka, T. NO_x storage performance at low temperature over platinum group metal-free SrTiO₃-based material. *ACS Appl. Mater. Interfaces* **2021**, *13*, 29482–29490. [[CrossRef](#)]
71. Tamai, K.; Hosokawa, S.; Kato, K.; Asakura, H.; Teramura, K.; Tanaka, T. Low-temperature NO oxidation using lattice oxygen in Fe-site substituted SrFeO_{3-δ}. *Phys. Chem. Chem. Phys.* **2020**, *22*, 24181–24190. [[CrossRef](#)]
72. Takamatsu, A.; Tamai, K.; Hosokawa, S.; Tanaka, T.; Ehara, M.; Fukuda, R. Oxidation and storage mechanisms for nitrogen oxides on variously terminated (001) surfaces of SrFeO_{3-δ} and Sr₃Fe₂O_{7-δ} perovskites. *ACS Appl. Mater. Interfaces* **2021**, *13*, 7216–7226. [[CrossRef](#)]
73. Ye, J.; Yu, Y.; Meng, M.; Jiang, Z.; Ding, T.; Zhang, S.; Huang, Y. Highly efficient NO_x purification in alternating lean/rich atmospheres over non-platinic mesoporous perovskite-based catalyst K/LaCoO₃. *Catal. Sci. Technol.* **2013**, *3*, 1915–1918. [[CrossRef](#)]
74. Qi, G.; Li, W. NO_x adsorption and reduction over LaMnO₃ based lean NO_x trap catalysts. *Catal. Lett.* **2014**, *144*, 639–647. [[CrossRef](#)]
75. Say, Z.; Dogac, M.; Vovk, E.I.; Kalay, Y.E.; Kim, C.H.; Li, W.; Ozensoy, E. Palladium doped perovskite-based NO oxidation catalysts: The role of Pd and B-sites for NO_x adsorption behavior via in-situ spectroscopy. *Appl. Catal. B* **2014**, *154*, 51–61. [[CrossRef](#)]
76. Li, X.G.; Dong, Y.H.; Xian, H.; Hernández, W.Y.; Meng, M.; Zou, H.H.; Ma, A.J.; Zhang, T.Y.; Jiang, Z.; Tsubaki, N.; et al. De-NO_x in alternative lean/rich atmospheres on La_{1-x}Sr_xCoO₃ perovskites. *Energy Environ. Sci.* **2011**, *4*, 3351–3354. [[CrossRef](#)]
77. Dong, Y.H.; Xian, H.; Lv, J.L.; Liu, C.; Guo, L.; Meng, M.; Tan, Y.S.; Tsubaki, N.; Li, X.G. Influence of synthesis conditions on NO oxidation and NO_x storage performances of La_{0.7}Sr_{0.3}MnO₃ perovskite-type catalyst in lean-burn atmospheres. *Mater. Chem. Phys.* **2014**, *143*, 578–586. [[CrossRef](#)]
78. Xie, W.; Xu, G.Y.; Zhang, Y.; Yu, Y.B.; He, H. Mesoporous LaCoO₃ perovskite oxide with high catalytic performance for NO_x storage and reduction. *J. Hazard. Mater.* **2022**, *431*, 128528. [[CrossRef](#)]
79. You, R.; Zhang, Y.; Liu, D.; Meng, M.; Zheng, L.; Zhang, J.; Hu, T. YCeZrO ternary oxide solid solution supported nonplatinic lean-burn NO_x trap catalysts using LaCoO₃ perovskite as active phase. *J. Phys. Chem. C* **2014**, *118*, 25403–25420. [[CrossRef](#)]
80. You, R.; Zhang, Y.; Liu, F.; Meng, M.; Jiang, Z.; Zhang, S.; Huang, Y. A series of ceria supported lean-burn NO_x trap catalysts LaCoO₃/K₂CO₃/CeO₂ using perovskite as active component. *Chem. Eng. J.* **2015**, *260*, 357–367. [[CrossRef](#)]
81. Onrubia-Calvo, J.A.; Pereda-Ayo, B.; Gonzalez-Velasco, J.R. Perovskite-based catalysts as efficient, durable, and economical NO_x storage and reduction systems. *Catalysts* **2020**, *10*, 208. [[CrossRef](#)]

82. Onrubia-Calvo, J.A.; Pereda-Ayo, B.; Bermejo-Lopez, A.; Caravaca, A.; Vernoux, P.; González-Velasco, J.R. Pd-doped or Pd impregnated 30% $\text{La}_{0.7}\text{Sr}_{0.3}\text{CoO}_3/\text{Al}_2\text{O}_3$ catalysts for NO_x storage and reduction. *Appl. Catal. B* **2019**, *259*, 118052. [[CrossRef](#)]
83. Onrubia-Calvo, J.A.; Pereda-Ayo, B.; De-La-Torre, U.; González-Velasco, J.R. Strontium doping and impregnation onto alumina improve the NO_x storage and reduction capacity of LaCoO_3 perovskites. *Catal. Today* **2019**, *333*, 208–218. [[CrossRef](#)]
84. Ding, Q.; Xian, H.; Tan, Y.; Tsubaki, N.; Li, X. Mesoporous SiO_2 -confined $\text{La}_{0.7}\text{Sr}_{0.3}\text{CoO}_3$ perovskite nanoparticles: An efficient NO_x adsorber for lean-burn exhausts. *Catal. Sci. Technol.* **2013**, *3*, 1493–1496. [[CrossRef](#)]
85. Qi, G.; Li, W. Pt-free, LaMnO_3 based lean NO_x trap catalysts. *Catal. Today* **2012**, *184*, 72–77. [[CrossRef](#)]
86. Onrubia-Calvo, J.A.; Pereda-Ayo, B.; Caravaca, A.; De-La-Torre, U.; Vernoux, P.; González-Velasco, J.R. Tailoring perovskite surface composition to design efficient lean NO_x trap $\text{Pd-La}_{1-x}\text{A}_x\text{CoO}_3/\text{Al}_2\text{O}_3$ -type catalysts (with A = Sr or Ba). *Appl. Catal. B* **2020**, *266*, 118628. [[CrossRef](#)]
87. Onrubia-Calvo, J.A.; Pereda-Ayo, B.; Cabrejas, I.; De-La-Torre, U.; González-Velasco, J.R. Ba-doped vs. Sr-doped LaCoO_3 perovskites as base catalyst in diesel exhaust purification. *Mol. Catal.* **2020**, *488*, 110913. [[CrossRef](#)]
88. Onrubia-Calvo, J.A.; Pereda-Ayo, B.; Urrutxua, M.; De La Torre, U.; González-Velasco, J.R. Boosting NO_x removal by perovskite-based catalyst in NSR–SCR diesel aftertreatment systems. *Ind. Eng. Chem. Res.* **2021**, *60*, 6525–6537. [[CrossRef](#)]
89. Albaladejo-Fuentes, V.; Sánchez-Adsuar, M.S.; Anderson, J.A.; Illán-Gómez, M.J. NO_x storage on $\text{BaTi}_{0.8}\text{Cu}_{0.2}\text{O}_3$ perovskite catalysts: Addressing a feasible mechanism. *Nanomaterials* **2021**, *11*, 2133. [[CrossRef](#)]
90. Yi, J.; Schroeder, M.; Weirich, T.; Mayer, J. Behavior of $\text{Ba}(\text{Co}, \text{Fe}, \text{Nb})\text{O}_{3-\delta}$ perovskite in CO_2 -containing atmospheres: Degradation mechanism and materials design. *Chem. Mater.* **2010**, *22*, 6246–6253. [[CrossRef](#)]
91. Peng, Y.; Si, W.; Luo, J.; Su, W.K.; Chang, H.Z.; Li, J.H.; Hao, J.M.; Crittenden, J. Surface tuning of $\text{La}_{0.5}\text{Sr}_{0.5}\text{CoO}_3$ perovskite catalysts by acetic acid for NO_x storage and reduction. *Environ. Sci. Technol.* **2016**, *50*, 6442–6448. [[CrossRef](#)]
92. Zhu, Y.; Zhou, W.; Yu, J.; Chen, Y.; Liu, M.; Shao, Z. Enhancing electrocatalytic activity of perovskite oxides by tuning cation deficiency for oxygen reduction and evolution reactions. *Chem. Mater.* **2016**, *28*, 1691–1697. [[CrossRef](#)]
93. Wen, W.; Wang, X.; Jin, S.; Wang, R. LaCoO_3 perovskite in $\text{Pt}/\text{LaCoO}_3/\text{K}/\text{Al}_2\text{O}_3$ for the improvement of NO_x storage and reduction performances. *RSC Adv.* **2016**, *6*, 74046–74052. [[CrossRef](#)]
94. Ciuparu, D.; Bensalem, A.; Pfeifferle, L. Pd–Ce interactions and adsorption properties of palladium: CO and NO TPD studies over Pd–Ce/ Al_2O_3 catalysts. *Appl. Catal. B* **2000**, *26*, 241–255. [[CrossRef](#)]
95. Nishihata, Y.; Mizuki, J.; Akao, T.; Tanaka, H.; Uenishi, M.; Kimura, M.; Okamoto, T.; Hamada, N. Self-regeneration of a Pd-perovskite catalyst for automotive emissions control. *Nature* **2002**, *418*, 164–167. [[CrossRef](#)]
96. Nishihata, Y.; Mizuki, J.; Tanaka, H.; Uenishi, M.; Kimura, M. Self-regeneration of palladium-perovskite catalysts in modern automobiles. *J. Phys. Chem. Solids* **2005**, *66*, 274–282. [[CrossRef](#)]
97. Ueda, A.; Yamada, Y.; Katsuki, M.; Kiyobayashi, T.; Xu, Q.; Kuriyama, N. Perovskite catalyst $(\text{La}, \text{Ba})(\text{Fe}, \text{Nb}, \text{Pd})\text{O}_3$ applicable to NO_x storage and reduction system. *Catal. Commun.* **2009**, *11*, 34–37. [[CrossRef](#)]
98. Li, X.G.; Chen, C.; Liu, C.; Xian, H.; Guo, L.; Lv, J.; Jiang, Z.; Vernoux, P. Pd-doped perovskite: An effective catalyst for removal of NO_x from lean-burn exhausts with high sulfur resistance. *ACS Catal.* **2013**, *3*, 1071–1075. [[CrossRef](#)]
99. Zhao, D.; Yang, Y.; Gao, Z.; Yin, M.; Tian, Y.; Zhang, J.; Jiang, Z.; Yu, X.B.; Li, X. Promoting NO_x reduction via in situ activation of perovskite supported Pd catalysts under alternating lean-burn/fuel-rich operating atmospheres. *Chin. J. Catal.* **2021**, *42*, 795–807. [[CrossRef](#)]
100. Ma, A.J.; Wang, S.Z.; Liu, C.; Xian, H.; Ding, Q.; Guo, L.; Meng, M.; Tan, Y.S.; Tsubaki, N.; Zhang, J.; et al. Effects of Fe dopants and residual carbonates on the catalytic activities of the perovskite-type $\text{La}_{0.7}\text{Sr}_{0.3}\text{Co}_{1-x}\text{Fe}_x\text{O}_3$ NO_x storage catalyst. *Appl. Catal. B* **2014**, *146*, 24–34. [[CrossRef](#)]
101. Artioli, N.; Matarrese, R.; Castoldi, L.; Lietti, L.; Forzatti, P. Effect of soot on the storage-reduction performances of $\text{PtBa}/\text{Al}_2\text{O}_3$ LNT catalyst. *Catal. Today* **2011**, *169*, 36–44. [[CrossRef](#)]
102. Castoldi, L. An overview on the catalytic materials proposed for the simultaneous removal of NO_x and soot. *Materials* **2020**, *13*, 3551. [[CrossRef](#)] [[PubMed](#)]
103. Yang, L.; Hu, J.; Tian, G.; Zhu, J.; Song, Q.; Wang, H.; Zhang, C. Efficient catalysts of K and Ce Co-doped LaMnO_3 for NO_x -soot simultaneous removal and reaction kinetics. *ACS Omega* **2021**, *6*, 19836–19845. [[CrossRef](#)] [[PubMed](#)]
104. Nuss, P.; Eckelman, M.J. Life cycle assessment of metals: A scientific synthesis. *PLoS ONE* **2014**, *9*, e101298. [[CrossRef](#)]